The Thesis Committee for Dhananjay Kumar
Certifies that this is the approved version of the following thesis:

Modeling Steam Assisted Gravity Drainage in Heterogeneous Reservoirs Using Different Upscaling Techniques

APPROVED BY
SUPERVISING COMMITTEE:

Supervisor:

Sanjay Srinivasan

Kamy Sepehrnoori

Modeling Steam Assisted Gravity Drainage in Heterogeneous Reservoirs Using Different Upscaling Techniques

by

Dhananjay Kumar, B.S.

Thesis

Presented to the Faculty of the Graduate School of

The University of Texas at Austin

in Partial Fulfillment

of the Requirements

for the Degree of

Master of Science in Engineering

The University of Texas at Austin

May 2014

Dedication

To my entire family, in the US and in India.

Acknowledgements

First and foremost, I would like to thank my supervisor, Dr. Sanjay Srinivasan. His influence on my career has been unmistakable and I owe a large part of my future success to him. The guidance he provided from the very first time during the summer internship hosted by the department all the way to the publication of this thesis has been invaluable. Additional gratitude goes to Dr. Kamy Sepehrnoori for agreeing to be my secondary reader on such short notice.

To all my office-mates and friends in the department, in particular Travis, Nnamdi, Hoon, Arti, Morteza, Brandon, Sayantan, Kwang Jin, Harpreet, Selin, Mayuri, Krupa, James, Henry, Dong, Michael, and Eric, I truly appreciate the friendship we developed over my time in Austin and the impact all of them had one way or another in my research. I owe an additional vote of gratitude for Travis, who as my roommate, had to put up with the occasional mess I left around the apartment.

I owe additional gratefulness to all my friends from back home in California and at UT. To all my friends at UT, I will hold all of the memories playing basketball together very dearly, none more than winning several intramural championship shirts. To my friends back home, I appreciate all of you keeping in touch with me after I moved away. I would especially like to give thanks to my closest friend, Nithya for the constant support and encouragement over my years in Austin.

Last but not least, I would like to thank my entire family, none more important than my parents, Bharath and Latha, and my younger brother, Mahesh, for their never-ending support throughout my pursuit of my MS. I only wish I was not bound by a few sentences to express how grateful and appreciative I am for their love and support throughout my entire life.

Abstract

Modeling Steam Assisted Gravity Drainage in Heterogeneous Reservoirs Using Different Upscaling Techniques

Dhananjay Kumar, M.S.E.

The University of Texas at Austin, 2014

Supervisor: Sanjay Srinivasan

This thesis presents different methods that improve the ability to relate the flow properties of heterogeneous reservoirs to equivalent anisotropic flow properties in order to predict the performance of the Steam Assisted Gravity Drainage (SAGD) process. Process simulation using full scale heterogeneous reservoirs are inefficient and so the need arises to develop equivalent anisotropic reservoirs that can capture the effect of reservoir heterogeneity.

Since SAGD is highly governed by permeability in the reservoir, effective permeability values were determined using different upscaling techniques. First, a flow-based upscaling technique was employed and a semi-analytical model, derived by Azom and Srinivasan, was used to determine the accuracy of the upscaling. The results indicated inadequacy of flow-based upscaling schemes to derive effective direction

permeabilities consistent with the unique flow geometry during the SAGD process. Subsequently, statistical upscaling was employed using full 3D models to determine relationships between the heterogeneity variables: k_v/k_h, correlation length and shale proportion. An iterative procedure coupled with an optimization algorithm was deployed to determine optimal k_v and k_h values. Further regression analysis was performed to explore the relationship between the variables of shale heterogeneity in a reservoir and the corresponding effective properties.

It was observed that increased correlation lengths and shale proportions both decrease the dimensionless flow rates at given dimensionless times and that the semi-analytical model was more accurate for cases that contained lower shale proportions. Upscaled heterogeneous values inputted into the semi-analytical model resulted in underestimation of oil flow rate due to the inability to fully account for the impact of reservoir barriers and the configuration of flow streamlines during the SAGD process.

Statistical upscaling using geometric averaging as the initial guess was used as the basis for developing a relationship between correlation length, shale proportion and k_v/k_h. The initial regression models did not accurately predict the anisotropic ratio because of insufficient data points along the regression surface. Subsequently a non-linear regression model that was 2nd order in both length and shale proportion was calibrated by executing more cases with varying levels of heterogeneity and the regression model revealed excellent matches to heterogeneous models for the prediction cases.

Table of Contents

List of Tables

List of Figures

Chapter 1: Introduction

As production from conventional resources of oil and gas slowly decrease, there is a growing need for global production from unconventional reservoirs. Heavy oil and bitumen are important classes of unconventional reservoirs and are expected to be major players in unconventional production. Current estimates of heavy oil and bitumen around the world, per the U.S. Geological Survey, are on the order of 3 billion barrels of original oil in place (OOIP) and 5 billion barrels OOIP, respectively (Meyer et al. 2007).

There is no clear criterion to differentiate between heavy oil and bitumen. To further complicate matters, the frequent reference to "extra-heavy oil" adds much to the confusion. One criterion for differentiating between heavy oil and bitumen is using their respective API gravities. Heavy oil has an API gravity between 10^0API and 20^0API inclusive and a viscosity greater than 100cp while bitumen has an API gravity less than 10^0API and a viscosity greater than 10,000cp (Meyer et. al. 2007).

The content of this work focuses on thermal recovery of bitumen from subsurface reservoirs. Furthermore, this thesis focuses on a popular method for extracting bitumen involving Steam Assisted Gravity Drainage (SAGD). SAGD involves the use of horizontally drilled injector and producer pair. The injector is located typically 3 – 5m above the producer. Steam is injected into the reservoir using the upper well and the heated bitumen/oil is drained through the bottom well as shown by Figure 1.1.

As steam is injected into the reservoir, it forms a chamber above the well pair and oil drains along the walls of the steam chamber. The SAGD process is a thermal enhanced oil recovery (EOR) method and is a gravity driven process, therefore involving relatively simple physics where the elevation of temperature due to the injection of steam reduces the viscosity of the bitumen dramatically, thus allowing the flow of oil.

Therefore, taller the steam chamber, more is contact of hot steam with the bitumen and consequently, larger the oil drainage rate. This was represented by Butler (1981) in his classic drainage equation.

However, as is the case with many other expressions to describe oil production, Butler's model assumes the simplest conditions, i.e. the reservoir is homogeneous and isotropic. Obviously, this is far from reality in most reservoirs and it remains unclear how anisotropy affects SAGD rates. Azom and Srinivasan (2011) point out that in most reservoirs, the steam-bitumen interface will be inclined at an acute angle to the principal axis of anisotropy during a typical SAGD process (Azom and Srinivasan 2011). As reservoirs increases in complexity, analytical models such as Butler's become more and more invalid and a proper modifications needs to be made to existing models to account for reservoir complexity.

1.1 MOTIVATION

Several researchers have indicated the difficulty in predicting the performance of the SAGD process using existing models including Azom and Srinivasan (2011). Some cases have reported under-prediction of performance while others have alluded to over-prediction using traditional expressions for oil rate and steam-oil-ratio. Therefore, a modified analytical model as described by Azom and Srinivasan (2011) is necessary to further enhance the understanding of SAGD and make improved predictions. Azom and Srinivasan's expression attempts to model the impact of permeability anisotropy on production. This work augments that work by providing a statistical technique for calculating spatially varying values of permeability anisotropy. It is demonstrated that such a technique can account for realistic variation in rock type in a reservoir, typically encountered in SAGD settings.

The starting point for most models in this report will be realistic variations in sand-shale distributions that then will be upscaled in order to calculate permeability anisotropy ratios—an aspect that Azom's work did not incorporate. The upscaling results will be in the form of statistical relationships between anisotropy and production that can then be used to assess the impact of anisotropy. Fully heterogeneous models at high resolution describing the spatial distribution of rock types are difficult to represent in field scale reservoir models because of the significant computational expense, Therefore, the assessment of equivalent anisotropic models that essentially mimic the fully heterogeneous system will allow us to make predictions efficiently and also enable us to assess the uncertainty associated with the predictions.

1.2 CONTRIBUTIONS OF THIS WORK

This thesis significantly enhances our understanding of the SAGD process from previous work and aims to assist in future SAGD modeling. The chapters of this report are divided accordingly.

Chapter 2 discusses the available literature related to the SAGD process and provides a thorough critique of the work.

In Chapter 3, we introduce the semi-analytical model as derived by Azom and Srinivasan and its application to the work presented in this thesis. In addition, we introduce the upscaling methods used to modify fully heterogeneous systems to an equivalent anisotropic model to reduce computation time in real-world cases. We show our results in matching the simulation results to the analytical model mentioned earlier.

Chapter 4 explores different statistical upscaling techniques to begin identifying relationships between stochastic shale distribution and permeability.

Chapter 5 explores statistical relationships between permeability anisotropy, shale correlation length and shale proportion. Multi-variable regression is introduced as a method to effectively determine relationships that can assist in understanding the relationship between heterogeneity and anisotropy.

We conclude the thesis in Chapter 6 with a review of the key research conclusions and future research issues.

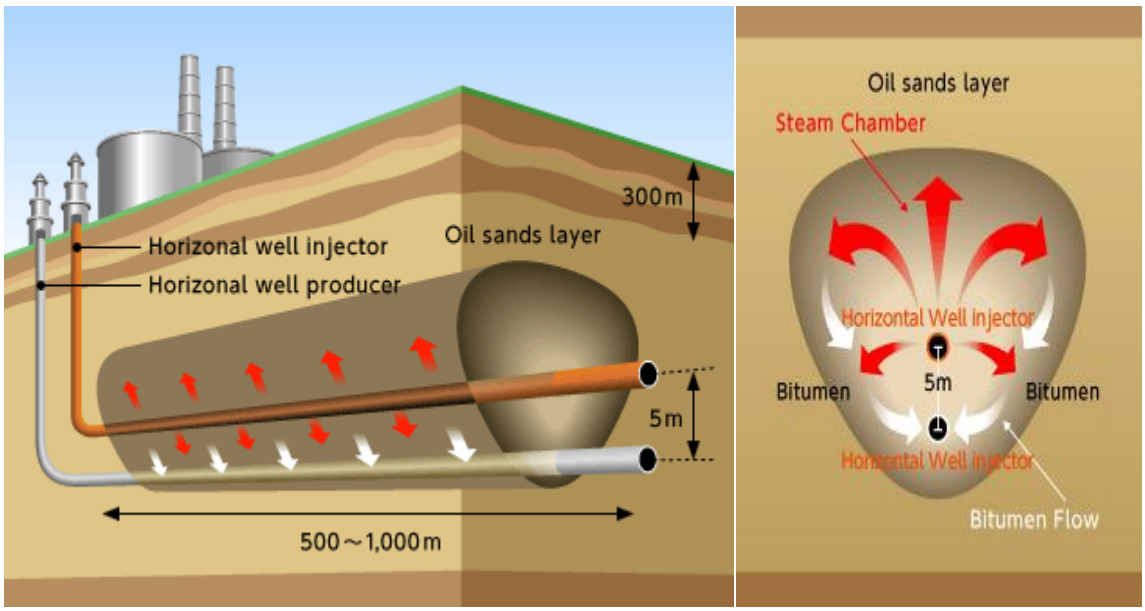

Figure 1.1: Schematic of a field scale application of the SAGD process with the general physics displayed on the front view by the right (courtesy of JAPEX).

Chapter 2: Literature Review

This chapter will feature a critique of past literature and research on the SAGD process with emphasis on prior efforts to model the effect of reservoir heterogeneity. We will look at works that accounted for permeability anisotropy in modeling the flow processes as this is the central theme of this thesis.

SAGD utilizes a pair of horizontal wells drilled above one another, where the top injector well injects steam into the reservoir. The injected steam rises by buoyancy and contacts the cold bitumen in the reservoir. The oil of reduced viscosity flows along the walls of the rising steam chamber. The heterogeneity of the reservoir will play a strong role in the rise of the steam and the flow of oil down to the producer. As such, modeling these types of processes using high resolution models is often computationally intensive and time consuming. Simple averaging techniques such as arithmetic, harmonic, geometric etc. are sometimes used to account for the heterogeneities and to produce equivalent anisotropic ratios for upscaled modeled but these in turn may sometimes be inadequate (Azom 2012). Therefore a robust upscaling technique is needed to account for the reservoir heterogeneity.

2.1 Modeling the Steam-Assisted Gravity Drainage (SAGD) Process

The first attempt to model the SAGD process was by Butler et al. (1981) where he assumed that the only significant transport mechanism was 1-D quasi-steady heat conduction ahead of the steam chamber front. This, coupled with Darcy's law gave the SAGD bitumen flow expression as derived by Butler.

$$q_o = \sqrt{\frac{2\phi \Delta S_o k g \alpha H}{m \nu_{os}}} \tag{2.1}$$

where

$$m = \left[\nu_{os} \int_{T_s}^{T_R} \left(\frac{1}{\nu_o} - \frac{1}{\nu_{oR}} \right) \frac{dT}{(T - T_R)} \right]^{-1} \tag{2.2}$$

governs the relationship between viscosity and temperature and typically vary from about 3 – 5 for typical heavy oil reservoirs (Butler, 1991). Essentially a higher value of this function implies that the viscosity-temperature curves changes less from the reservoir to steam temperature.

Equation 2.1 states that the bitumen drainage rates is directly proportional to the square root of reservoir permeability (k), thermal diffusivity (α), porosity (ϕ), mobile oil saturation (ΔS_o), and the thickness of the reservoir (H). It is however, inversely proportional to the square root of the Butler viscosity parameter (m), and the kinematic viscosity of bitumen at steam temperature (ν_{os}).This model suggests a simple method to improve bitumen flow rates—by increasing factors such as the residual oil saturation S_{or}, the and/or decreasing the values of the denominator terms such as the operating temperature.

Equation (2.1) predicts that the oil rate is constant and the expression is only valid when the steam chamber has grown to the top of the formation and is growing laterally till it reaches the boundary of the reservoir. This phase is known as the horizontal steam

chamber growth phase (Llaguno et al., 2002). Furthermore, Butler's equation (2.1) relating recovery to various reservoir and fluid parameters was derived for a purely isotropic permeable medium, it could not account for directional heterogeneities. One way to introduce heterogeneities in the system is by extending the rate expression of Butler to include the permeability anisotropy information computed by upscaling the heterogeneous reservoir model.

2.1.1 The Effect of Anisotropy

It is already well known and documented that permeability anisotropy has a strong effect on recovery processes like SAGD that utilize horizontal wells (Peaceman, 1993). Alali et al. (2009) used geometric averaging of the vertical and horizontal permeabilities of a reservoir to develop their semi-analytical model, however they demonstrated the validity of their model only over a very small range of cases. Azom and Srinivasan (2011) found that as the steam chamber rises to the top of the formation in a inverted triangular shape, the influence of the vertical permeability on bitumen rates decreases while the influence of the horizontal permeability on bitumen rates increases therefore implying that the influence of anisotropy is time dependent.

To show the influence of anisotropy, Sharma et al. (2002) used a thermal simulator to simulate the SAGD process for various different k_v/k_h ratios and found that the rate is generally reduced for a decreasing k_v/k_h ratio and also found that the overall shape of the curves, when compared to one another, appear shifted in time. This plot, Figure 9 from their publication, is shown below in Figure 2.1.

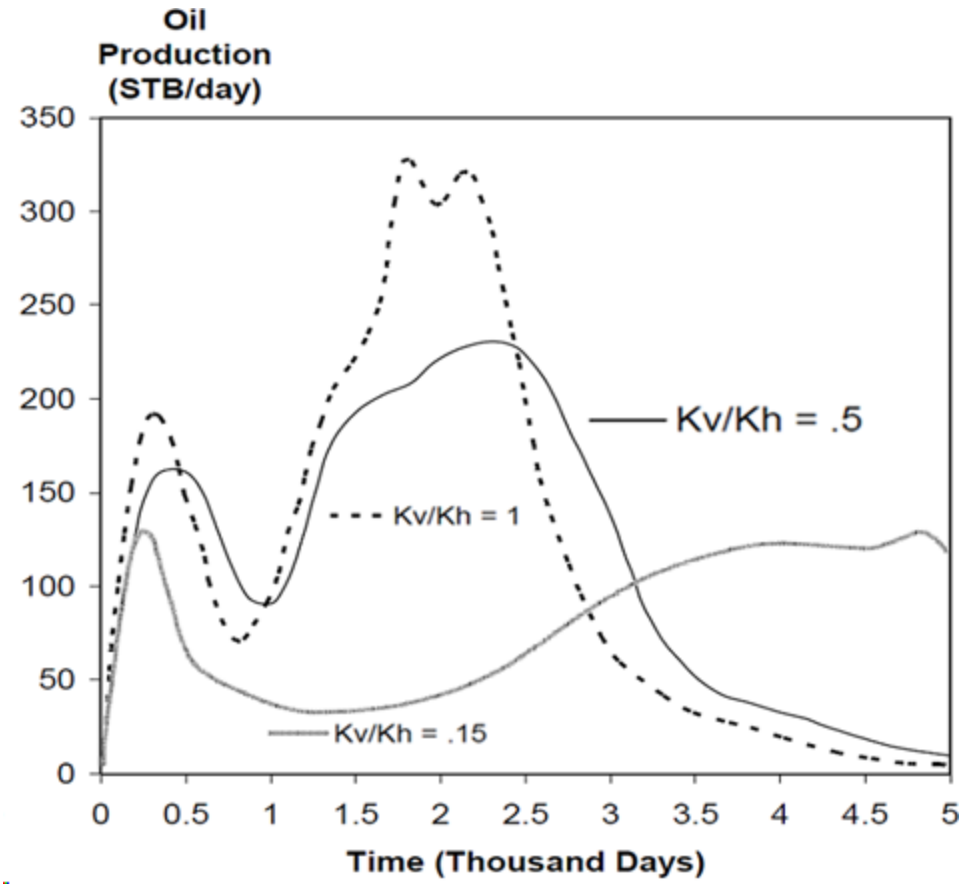

Figure 2.1: SAGD oil production rates for different k_v/k_h ratios showing the effect of anisotropy (courtesy of Sharma et al., 2002, SPE)

McLennan and Deutsch (2006) found that the flow performance during SAGD is heavily dependent and sensitive to the spatial distribution of permeability and the contrast between vertical and horizontal permeability. Additionally, Barillas et al. (2006) determined that heterogeneity as well as vertical permeability had a major influence on SAGD recovery. One particular conclusion that they drew however was that cumulative oil recovery increased with a decrease in vertical permeability. Naturally, this is counter-intuitive when compared to the results in Sharma et al. (2002). The contrary conclusions drawn these authors are a prime example of the difficulty in comparing results from

analytical models and semi-analytical models with numerical simulations. Barillas et al. postulated that their counter-intuitive results were a result of steam breakthrough which is not accounted for in any analytical or semi-analytical models and can drastically alter the physics behind the process.

Another observation of Sharma et al. was that there was an upper limit to the vertical permeability for their reservoir and that beyond that point there was no influence on the cumulative oil recovery, suggesting that there might be a specific combination of parameters which would render anisotropy unimportant and meaningless in terms of its impact on SAGD performance. This is further supported by Kisman and Yeung (1995) who found that lowering k_v/k_h reduced production rates by approximately 32% initially after which rates would gradually increase to about 8% of the fully homogeneous (isotropic) base case after 8 years.

Anisotropy in reservoir models can be attributed to the presence of stochastically occurring streaks of shale barriers (Begg and Chang, 1985) laterally present in porous media (Deutsch, 2010). These shale barriers typically have dimensions that are smaller than the size of an average grid block in a simulation and the resulting k_v/k_h ratio can be calculated for these systems by considering the streamline path of fluid as it navigates through a medium entrenched with stochastic shale streaks (Haldorsen and Lake, 1984). Shale streaks that begin to exceed the size of one grid block can significantly affect the SAGD process (Chen et al., 2008); (Le Ravalec et al., 2009); (Shin and Choe, 2009).

To account for such heterogeneity and the possibility of shale barriers in a system, Kamath et al. (1993) developed a 2D SAGD model modified from Butler's updated SAGD model (1985). Their findings revealed that with a given amount of heterogeneity in a reservoir, the possibility for improved recovery would increase if the producer well was in a higher permeability region instead of a lower one.

Azad (2012) was the first to present a model that captured the effect of geomechanics on SAGD performance and to study the changes in oil saturation ahead of the steam chamber front. They called this model Geomechanical Azad Butler (GAB) model and it only studied the geomechanical effects during SAGD and therefore did not produce any results pertinent to the effect of anisotropy on SAGD flow rates.

2.1.2 Introduction to Modified Analytical Model

Azom and Srinivasan (2011) modified Butler's original equation for flow rate during SAGD by re-deriving the flow equations using the velocity vector resolved along the principal axes of the anisotropy. This resulted in a flow rate equation that is similar to Butler's original equation but with the permeability term k in Equation 2.1 replaced by an effective permeability due to the anisotropy present in the reservoir, k_{eff} as shown in Equation 2.3. Isotropy of permeability can be geometrically represented as a sphere where the radii equated to permeability are the same in all directions, whereas anisotropy can be represented as an ellipsoid (or ellipse in 2D) with permeability different in different directions. Assuming that the principal directions of permeability anisotropy are in the horizontal and vertical directions, they resolve the oil flux at the steam chamber wall that is at an oblique angle to the axes of anisotropy (as shown in Figure 2.2) in order to come up with the rate expression:

$$q_o = \sqrt{\frac{2\phi \Delta S_o k_{eff} g \alpha_T H}{m \nu_{os}}} \tag{2.3}$$

Where ΔS_o is the mobile oil saturation, α is the thermal diffusivity, H is the thickness of the reservoir or bitumen column, m is the Butler parameter and ν_{os} is the bitumen kinematic viscosity at steam temperature. Furthermore, because the angle subtended by the steam chamber to the principal directions of anisotropy changes with time, Azom and Srinivasan (2011) derive an expression for the change in steam chamber width with time that will obey the physics of the SAGD process. The derived expression for rate is such

that it approaches the isotropic limit as time progresses and hence they conclude that the effect of anisotropy is minimized as the process continues.

One of the principal assumptions in Butler's original derivation is that the steam chamber conforms to an inverted triangular shape. The assumption of an inverted triangle shape is essential for the derivation of Azom and Srinivasan's model, shown below. Additionally, only the horizontal growth phase is considered since it is the most likely to conform to the inverted triangular shape.

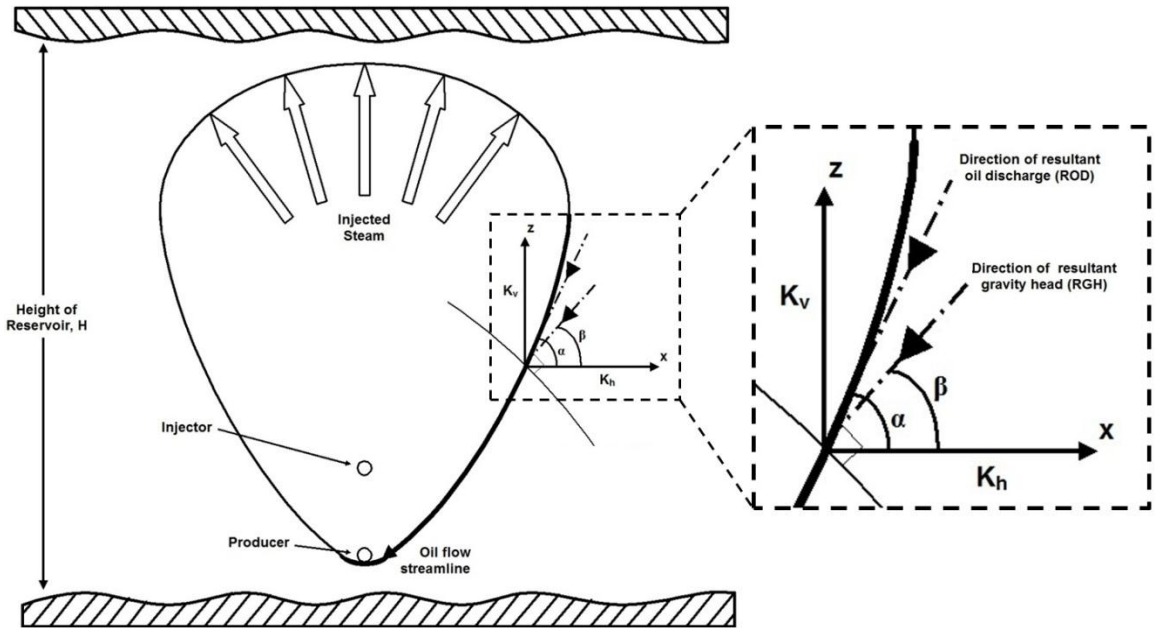

Figure 2.2: Diagram of typical 2D SAGD process with the formation of steam chamber and important oil drainage directions (courtesy of Azom and Srinivasan 2011)

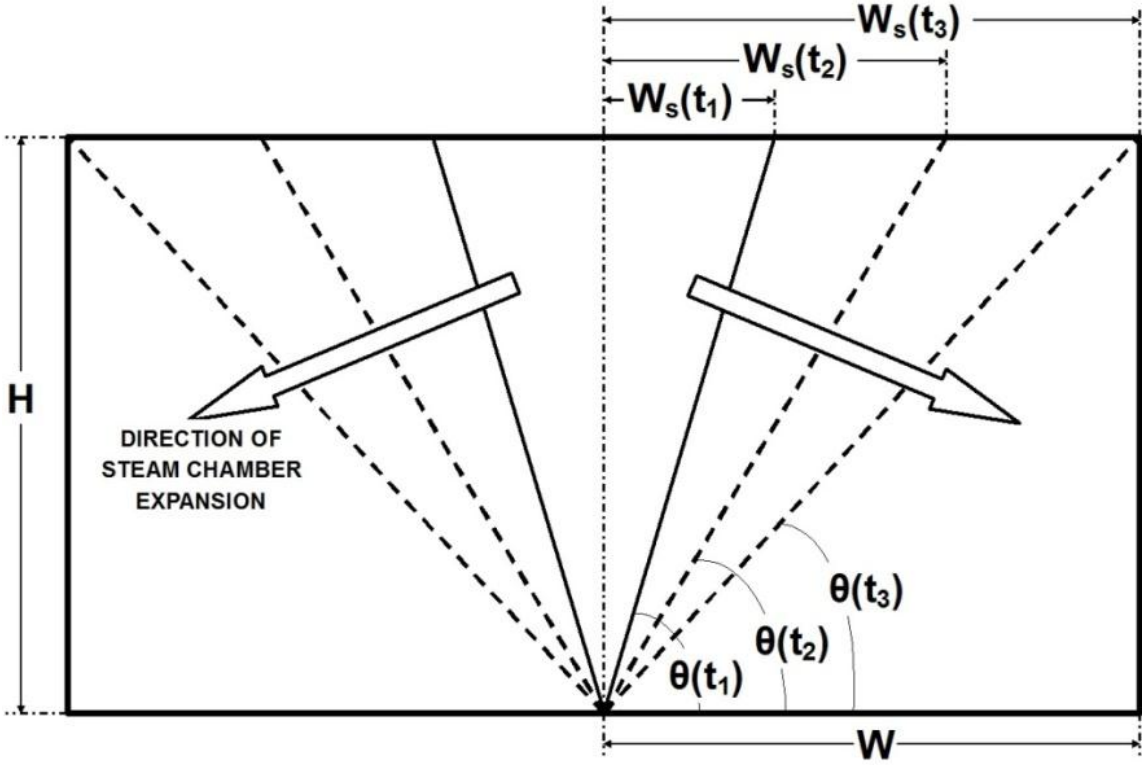

Figure 2.3: Theoretical SAGD steam chamber spreading during the horizontal growth phase (courtesy of Azom and Srinivasan 2011)

Figure 2.3 shows the change in chamber width and hence the repose angle J as time progresses. An expression for the change in the steam chamber angle as a function of time can be written as:

$$\theta = \theta(t) = \arctan\left(\frac{H}{W_s(t)}\right) \tag{2.4}$$

Azom and Srinivasan found that as $W_s \to W$, the influence of vertical permeability on the drainage of the bitumen along the steam chamber walls decreases whereas the influence of the horizontal permeability increases. Therefore, the results for oil rate obtained using

their expression is expressed in dimensionless form by dividing the oil rate for the anisotropic case by the corresponding isotropic flow rate corresponding to $k_v/k_h \to 1$.

Azom and Srinivasan (2011) referenced Das (2013) to describe their two choices for representing their model of anisotropy. Resolution of the resultant gravity head vector (Figure 2.2) on the axes of the permeability anisotropy results in:

$$k_{eff_{RGH}} = k_v \sin^2\theta + k_h \cos^2\theta \tag{2.5}$$

Whereas resolving the resultant oil drainage vector (Figure 2.2) on the axes of anisotropy results in:

$$\frac{1}{k_{eff_{ROD}}} = \frac{\sin^2\theta}{k_v} + \frac{\cos^2\theta}{k_h} \tag{2.6}$$

The RGH model assumes that the bitumen flow occurs in the direction perpendicular to the equipotential surface while the ROD model assumes that the bitumen flow occurs tangential to the steam chamber interface.

This work will focus on the use of the RGH model for anisotropy as gravity is the dominant physical drive affecting the process and in the case of a stair-stepping steam profile (because of the presence of shale barriers) it is difficult to identify and resolve the resultant oil drainage vector. All analytical, and even semi-analytical models, implicitly assume the RGH model because of the ability to obtain bitumen rates as a function of the resultant gravity potential gradient in the direction parallel to the steam chamber interface (Azom and Srinivasan 2011). The detailed derivation for the ROD model can be found in Azom (2013). By substituting Equation (2.5) into Equation (2.1) we get:

$$q_{o_{RGH}} = \sqrt{\frac{2\phi\Delta S_o \left(k_v \sin^2\theta + k_h \cos^2\theta\right) g\alpha_T H}{m\nu_{os}}} \tag{2.7}$$

Writing $W_s(t)$ in Equation (2.4) at any particular time as W_s, we come up with:

$$\cos^2\theta = \frac{W_s^2}{W_s^2 + H^2} \tag{2.8}$$

$$\sin^2\theta = \frac{H^2}{W_s^2 + H^2} \tag{2.9}$$

Finally, substituting Equations 2.8 and 2.9 into Equation (2.7) we get the following model derived by Azom and Srinivasan (2011):

$$q_{o_{RGH}} = \sqrt{\frac{2\phi\Delta S_o \left(\frac{k_v H^2 + k_h W_s^2}{W_s^2 + H^2}\right) g\alpha_T H}{m\nu_{os}}} \tag{2.10}$$

To compare across different reservoirs with different proportions of shale and varying lengths, non-dimensionalizing $q_{o_{RGH}}$ is necessary. To do so, dividing $q_{o_{RGH}}$ by the equivalent isotropic bitumen rate will result in a non-dimensional form of bitumen rates that will be then evaluated against dimensionless time t_D:

$$q_{D_{RGH}} = \frac{q_o}{q_{o_{kv/kh=1}}} \tag{2.11}$$

$$t_D = \sqrt{\frac{k_h g\alpha_T}{\phi\Delta S_o m\nu_{os} H^3}}\, t \tag{2.12}$$

2.2 STATISTICAL UPSCALING

The validation of Azom and Srinivasan's model, as will be discussed in Chapter 3, requires a method for upscaling a fully heterogeneous model to a corresponding anisotropic model using a flow-based method.

Given the spatial distribution of shale an effective anisotropy ratio can be computed using a flow-based upscaling method (Durlofsky 1991). The upscaling procedure for the determination of equivalent permeability involves the solution of the Laplace equation for pressure within the reservoir domain subject to periodic boundary conditions. A pressure gradient is imposed in the flow direction and a linear pressure profile on the two other opposite faces. This variation results in a non-symmetrical permeability tensor taking into account the cross-flow term. Symmetric, positive definite equivalent permeability tensors are obtained by the procedure.

However, conventional physics-based upscaling techniques such as Durlofsky's method, make several assumptions regarding boundary conditions at the top of the reservoir, single phase fluid flow etc. that are inconsistent with the actual conditions during the SAGD process. Effective permeability can also be computed using statistical schemes. The three statistical methods used for upscaling are the three Pythagorean means: arithmetic, geometric and harmonic. The effective permeability as calculated by the three different methods is given by

$$k_{avg-eff} = \frac{1}{n}\sum_{i=1}^{n} k_i \tag{2.13}$$

$$k_{geo-eff} = \sqrt[n]{\prod_{i=1}^{n} k_i} \tag{2.14}$$

$$k_{har-eff} = \frac{1}{\frac{1}{n}\sum_{i=1}^{n}\frac{1}{k_i}} \tag{2.15}$$

Each method has its advantages and disadvantages. The arithmetic mean is known to be sensitive to extreme outliers, while the geometric mean gives more weight to smaller values and less weight to higher values and the harmonic mean of a data set is always the lowest of the three.

Using statistical averaging techniques to estimate an effective permeability value for the entire reservoir is a common method that has been practiced in the industry for some time. Furthermore, Warren and Price (1961) first determined that using the geometric mean of individual permeability values in the entire reservoir is an effective way to estimate the overall reservoir heterogeneity. They believed that while all porous media are heterogeneous on the microscopic level, only macroscopic fluctuations need consideration since reservoir mechanics are based on macroscopic quantities. Jensen (1991) stated that the use of geometric averaging to calculate the effective permeability is appropriate under certain conditions. Matheron (1967), Bakr et al. (1978), Gutjahr et al. (1978) and Dagan (1979, 1981) also studied this and found that geometrically averaging can be effective when permeabilities are log-normally distributed with low variance.

Deutsch (1987) summarized in his dissertation that the effective permeability in three dimensions is bounded by the harmonic mean as a lower limit and the arithmetic

mean as an upper limit. The effective permeability can then be seen as a power average with a power value $-1 \leq \omega \leq 1$ summarized by Equation 2.16.

$$K_{eff-pwr} = \left[\sum_{i=1}^{i=n_i} p_i \bullet k_i^{\,w} \right]^{\frac{1}{w}} \tag{2.16}$$

Where the distribution of permeability is split into n_e modes and each permeability datum could represent a class at the limit. In this expression p_i is the volume fraction of class *i*, k_i is the permeability of class *i* and ω is the power of averaging.

In this thesis, we have explored several models that account for heterogeneity and anisotropy. This work will extend some aspects of the research undertaken by Azom (2013) and expand beyond the limitations of the analytical model that was derived by Azom and Srinivasan (2011). Chapter 3 will expand on the model derived by Azom and Srinivasan and will attempt to validate it. Chapter 4 will conduct simulations for full 3D heterogeneous as well as anisotropic reservoirs while determining relationships between heterogeneity due to shale barriers exhibiting various correlation lengths and corresponding anisotropic permeability parameters. Chapter 5 will use multi-variable regression to determine relationships between k_v/k_h to cumulative oil recovery for various shale correlation lengths and shale proportions.

Chapter 3: Modeling the Effect of Permeability Heterogeneity on SAGD Using a Semi-Analytical Approach

The SAGD process is used to produce heavy oil/bitumen by injecting steam into the reservoir with a horizontal well pair typically spaced 5-10m apart, with the producer at the bottom. As a gravity driven process, SAGD involves relatively simple physics where the injection of steam creates a high temperature steam chamber allowing for the viscosity of oil to dramatically decrease along the walls of the chamber and drain downwards toward the producer. Hence, the taller the steam chamber, the larger the oil drainage rate. Butler's model (Butler 1985) accounts for steam chamber growth and oil recovery during SAGD, but it assumes the reservoir is both homogenous and isotropic. This is far from the case for most real reservoirs because the steam chamber interface will most times grow at an incline to the principal axes of permeability anisotropy during a typical SAGD process. Azom and Srinivasan showed that the effect of anisotropy is time dependent and there exists a given time beyond which it ceases to have any effect on SAGD rates (Azom and Srinivasan 2011).

Several authors have attempted to better understand the SAGD process and account for to the effect of permeability heterogeneity on recovery, not included in the original Butler model (Najeh et al. 2009, Duong et al. 2008). However, the inadequacies of these models together with the requirement to support operational considerations such as spacing of wells and the amount of steam injected has led to the routine use of numerical simulation models to predict its recovery. The benefit of such numerical models is that they can be used to design field implementations of the SAGD process, but

the challenge rests in their inadequacy to generate and test comprehensive theories that operate at different scales, a key strength of analytical approaches. Previous semi-analytical models have either been too complex to justify their use (Kamath et al. 1993) or have included assumptions that are difficult to justify (Sharma & Gates 2010). In this chapter, we explore the application of a simple semi-analytical model developed by Azom and Srinivasan (2011), to investigate physical characteristics of the SAGD process that have been inadequately studied in the past and to provide recommendations for further modification of the Azom and Srinivasan model.

3.1 ANALYTICAL MODEL

The model developed by Azom and Srinivasan is a modification of Butler's equation (2.1) to account for the impact of anisotropic permeability. Based on the critical assumption of a steam chamber in the shape of an inverted triangle, the effective permeability affecting the growth of the steam chamber is developed by resolving the vector along which the oil drainage occurs along the principal axes of anisotropy, The resolved equivalent drainage flux is then incorporated into the oil rate expression. As discussed in the previous chapter, there are two methods for calculating this effective permeability based on the resolution of the oil flow stream lines at the edge of the steam chamber - resultant gravity head (RGH) and resultant oil discharge (ROD). The ROD model assumes that bitumen flow occurs tangential to the steam chamber interface while the RGH model assumes that bitumen flow occurs in the direction perpendicular to the equipotential surface. Resolution of the oil flow vector along these two directions yields

the expressions that capture the effective permeability as shown by (2.5) and (2.6) (Azom and Srinivasan 2011).

Azom does not provide a recommendation on which model to use, but in this chapter, the RGH model will be used. Steam chamber angle, θ, can be estimated as a function of time once the steam chamber has reached the overburden and begins growing horizontally, as shown in (2.4). The derivation of this expression can be seen in Chapter 2, with the final expression shown by (2.10).

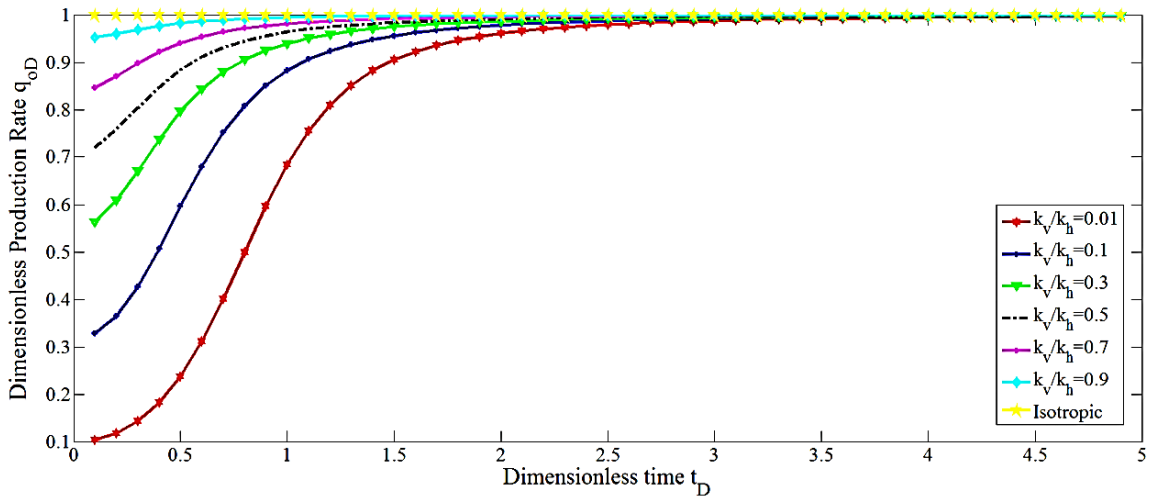

Figure 3.1: Plot of dimensionless rate vs. dimensionless time for the RGH model (courtesy of Azom and Srinivasan 2011)

The dimensionless oil rate predicted by the RGH model as a function of dimensionless time for various values of the k_v/k_h ratio is shown in Figure 3.1. The dimensionless oil rate is obtained by standardizing the oil rate for the anisotropic case by the corresponding rate for the isotropic case. The figure shows that as the k_v/k_h decreases, it takes longer for

the effect of anisotropy to dampen and approximate the rate corresponding to the isotropic case.

3.2 RESERVOIR AND SIMULATION MODEL DEVELOPMENT

Several reservoir models with shale lenses within a consolidated sand matrix whose parameters are summarized in Table 3.1 were simulated using CMG STARS. Heterogeneities were introduced in the form of low permeability lenses. The lenses are characterized by a correlation length that relates to the horizontal extent of the streak. Multiple reservoir realizations for each correlation length were created in Stanford Geostatistical Modeling Software (SGeMS) using sequential indicator simulation. An example realization can be seen in Figure 3.2. The correlation lengths varied from short lengths, 5m, to mid-range lengths, 35m. The particular value for the limit of the mid-range structure was chosen, because, as the correlation length approached the half-width of the reservoir, the lenses coalesced and created an unbroken barrier across the reservoir. Therefore, low permeability lenses longer than a quarter of the reservoir width were not studied.

Table 3.1: Reservoir Parameters

Porosity	0.3	Reservoir Temp.	60^{o}C
Permeability, Sand	3000 md	Steam Temp.	225^{o}C
Permeability, Shale	10 md	Steam Quality	0.8
Viscosity (CMG 2011)	$Ae^{B/T}$	Height	50 m
A	1.95E-11	Width	150 m
B	11500.1	Grid Size	1mx1m

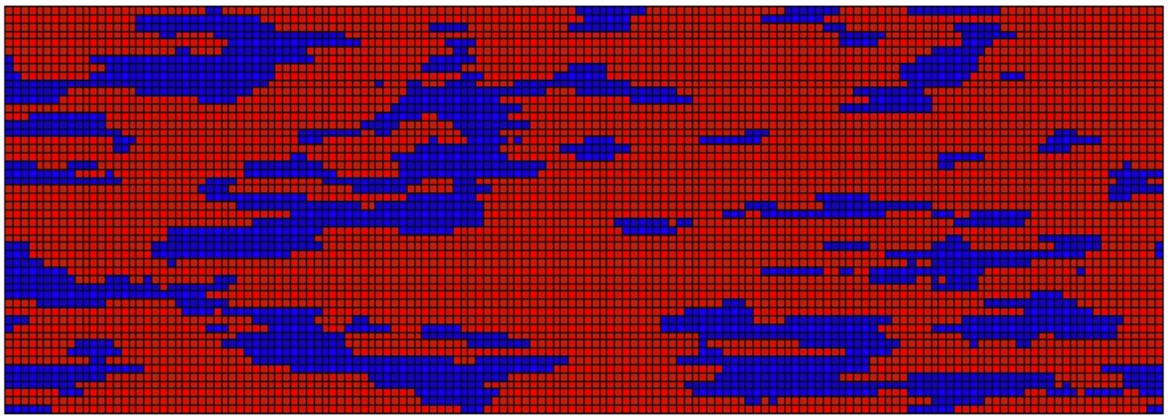

Figure 3.2: Heterogeneous model for shale with shale lens length of 15m and frequency of 30%.

3.3 RESULTS AND DISCUSSION

The results of the numerical simulation for an anisotropic case and that for the corresponding isotropic case are shown in Figure 3.3 below. This realization had a vertical permeability of 351 md and a horizontal permeability of 816 md.

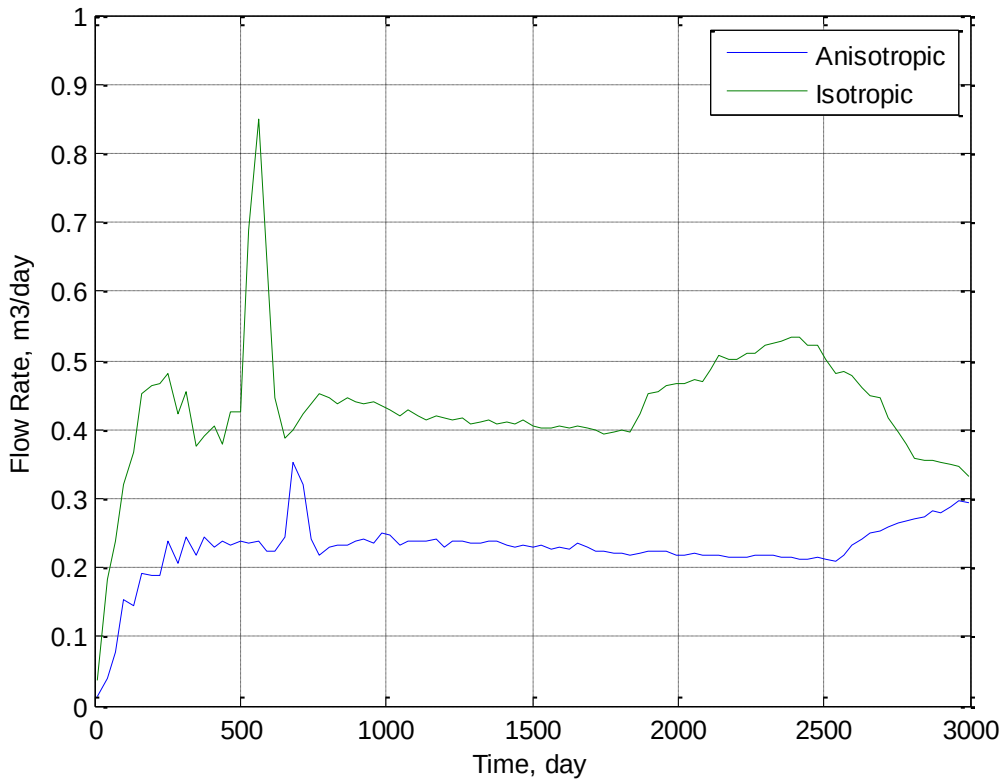

Figure 3.3: Flow rate over time, lens length of 15m and lens frequency of 30%

Given the spatial distribution of shale an effective anisotropy ratio was computed and used to compare the numerical simulation result for oil rate with the corresponding prediction using Azom's model. For each realization of shale distribution, the effective horizontal and vertical permeability were calculated using a flow-based upscaling method (Durlofsky 1991). The upscaling procedure for the determination of equivalent

permeability involves the solution of the Laplace equation for pressure within the reservoir domain subject to periodic boundary conditions. A pressure gradient is imposed in the flow direction and a linear pressure profile on the two other opposite faces. This variation results in a non-symmetric permeability tensor taking into account the cross-flow term. Symmetric, positive definite equivalent permeability tensors are obtained by the procedure. It is important to note that the upscaling code does not uniquely differentiate between correlation length and frequency, which often results in overlapping results corresponding to several cases. Figure 3.4 displays this overlap that can occur between cases with different correlations. Although the flowrate profile at the later times overlap, the initial rates differ between the two cases and that might be due to the different rate at which the steam rises in the presence of shale of different correlation lengths.

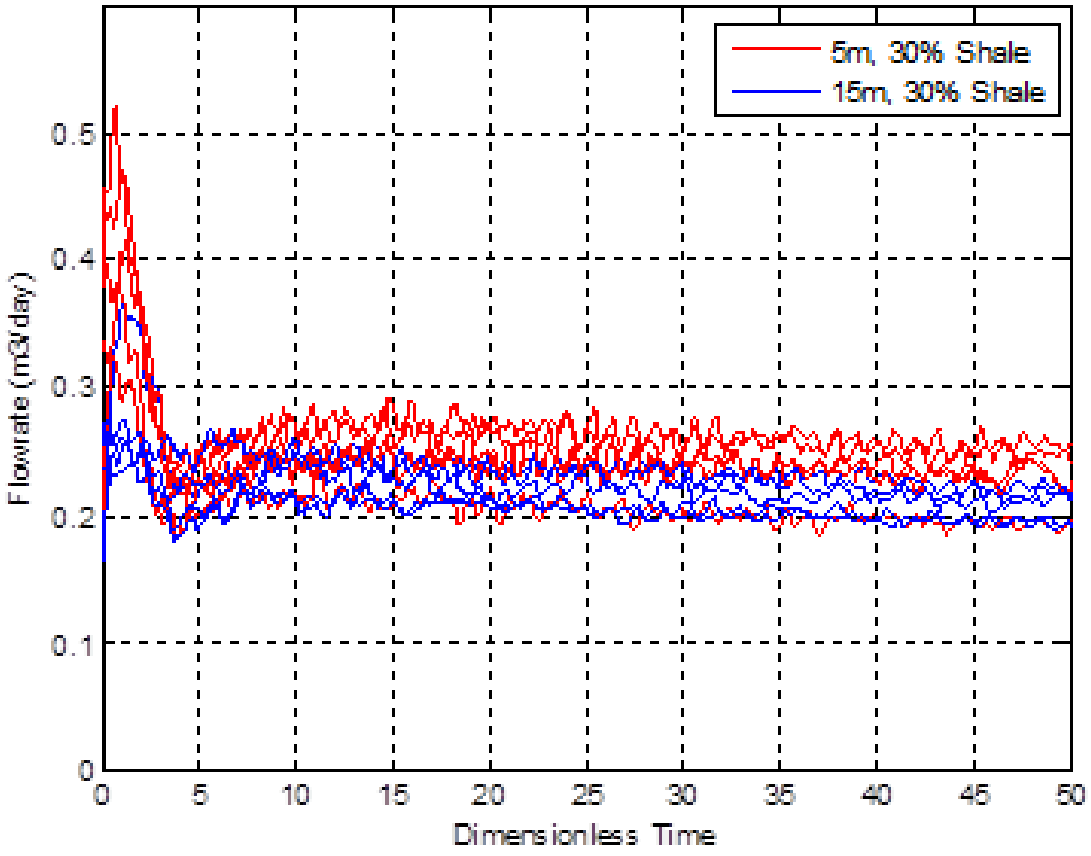

Figure 3.4: Production response for different anisotropic correlation lengths

3.3.1 Non-dimensionalizing variables

Once the effective permeability values were obtained, anisotropic computer models were created using the anisotropic permeability values and simulated in CMG STARS. The flow rates from these simulations are non-dimensionalized by dividing by the flow rate from the anisotropic model with that from a homogeneous reservoir with permeability equal to the horizontal permeability of the anisotropic model. This yields dimensionless flowrate consistent with Equation 2.11 in Chapter 2. In order to compute

the dimensionless flowrate, $q_{D_{RGH}}$ accurately, care was taken to make sure that the t_D was corresponding to the same relative position of the steam chamber in both the anisotropic and homogeneous cases. An algorithm was developed in Microsoft Excel's Visual Basic for Applications (VBA) that could identify exact matches between the anisotropic and homogeneous cases. t_D is based on the triangular-shape of the steam chamber, and is set to zero at the moment the steam chamber hits the roof of the reservoir layer and resumes horizontal growth. The parameters used to generate the shale realizations, resulting K_v/K_h values along with the VBA algorithm are located in the Appendix.

3.3.2 Accounting for Deviations from Butler's Model

Azom's model for the effect of permeability anisotropy on oil rate is predicated on the growth of the steam chamber in the form of a reverse cone. Naturally, in the presence of shale barriers, the steam chamber will not have the ability to rise in an inverted triangular shape, with the steam rise showing patterns similar to that shown in Figure 3.5, thus the need for anisotropy that can correctly represent the growth of the steam chamber in the presence of shale. The deviation of the steam chamber from the classical shape assumed in the model by Butler is minimized when the full heterogeneous reservoir is upscaled to contain an effective permeability capturing the heterogeneous behavior as shown in Figure 3.6.

In order to take into account the deviation of the chamber from the classical shape assumed by Butler (1985) and Azom and Srinivasan (2011), the width of the steam chamber as simulated is recorded at unique time intervals and used for calculating the

steam chamber width W_s in Equation 2.10. Another assumption in Azom's model is that there is a step change in water saturation from S_{or} (inside the steam chamber) to S_{oi} past the steam front. In the flow simulation however, the steam front is smeared due to numerical dispersion. Thus, in order to compare the numerical simulation results with Azom's model, the average oil saturation within the steam chamber is calculated at a few discrete times and used to calculate ΔS_o that is in turn used in the oil rate expression (2.10). To do so, an algorithm was developed in VBA that would calculate the saturation of oil inside the steam chamber while nulling all other values to increase accuracy of the calculation within the steam chamber. To obtain specific values of the saturation profile, the RESULTS 3D feature in CMG STARS™ was utilized.

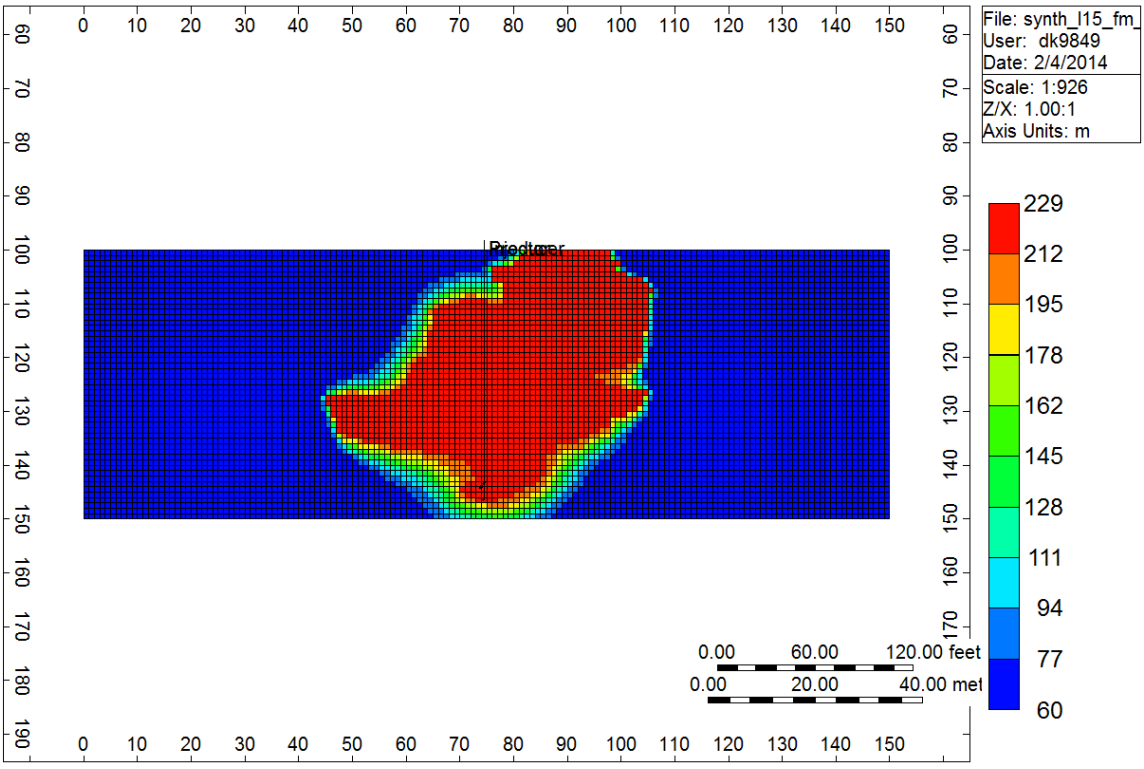

Figure 3.5: Distorted Steam Chamber Growth in Reservoir with Shale Barriers

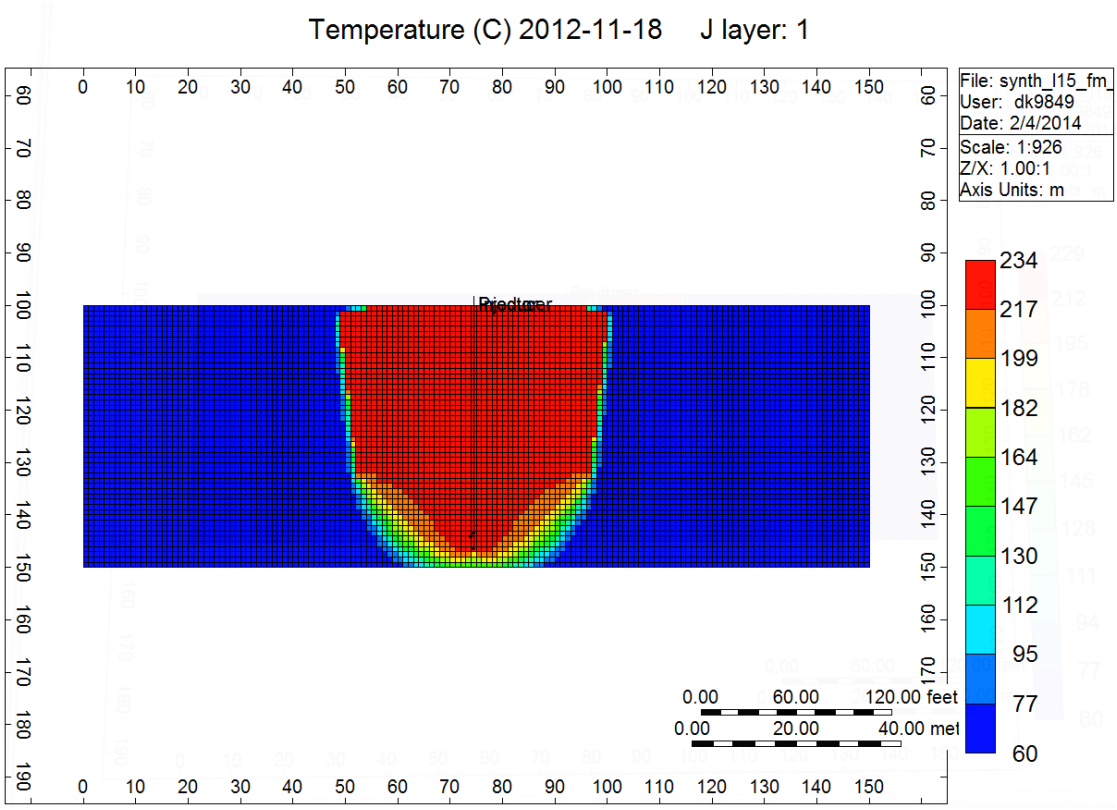

Figure 3.6: Anisotropic reservoir with steam chamber adhering to Butler's concept

3.3.3 Some Observations based on the Analytical Rate Expressions

The correlation length and volumetric concentration of the shale lenses impacts the upscaled permeability values and, ultimately, the flow rates. In Figure 3.7, the dimensionless flow rate from the anisotropic simulation as well as predictions using Azom's analytic model are plotted for a range of shale lens dimensions. Figure 3.7, displays the effect of an increased shale proportion on oil rate, independent of lens size. As anticipated, the flow rates show a dependence on both correlation length and the frequency of lenses.

A longer correlation length of shale lenses yielded a lower k_v/k_h ratio and a slower recovery rate. Higher shale concentrations (30%) caused the analytical model to predict flow rates that were higher than the simulation results. Furthermore the flow rate curves of both the anisotropic simulation and analytic model approach the homogeneous flow rate at a later time. In all the numerical simulation cases, there is an initial mismatch between the numerical simulation results and the analytical model results. This is due to the difficulty in pin-pointing the onset of the horizontal growth phase from the numerical simulation results. Differences in the frequency of low permeability lenses had an analogous effect on the flow rates. A lower shale frequency results in higher k_v/k_h ratio, causing both the analytic model and anisotropic results to have higher flow rates at a given time. In addition, as the frequency of shale lenses increases, the match between the analytical model and the simulation results decreases. This can be due to the change in physics as the amount of shale increases and the slow migration of steam by skirting around the shale barriers.

Because Azom and Srinivasan's model is only a modification of Butler's original model, it also assumes a classical inverted steam chamber in the derivation of the rate expression. As the shale concentration and/or length increase however, the steam chamber growth deviates away from the ideal model and this in-turn makes the Butler model, and correspondingly, the Azom and Srinivasan model less accurate. This is displayed in Figure 3.8. Figure 3.9 displays a relatively good match between the simulation results and the analytical model due to the low concentration of shale lenses.

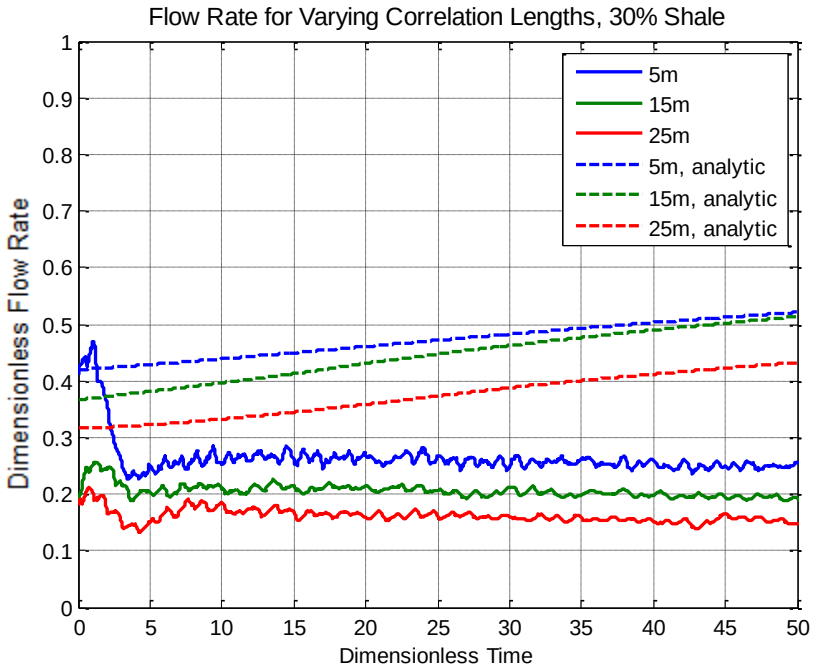

Figure 3.7: Dimensionless flow rate varying correlation length, 30% shale proportion

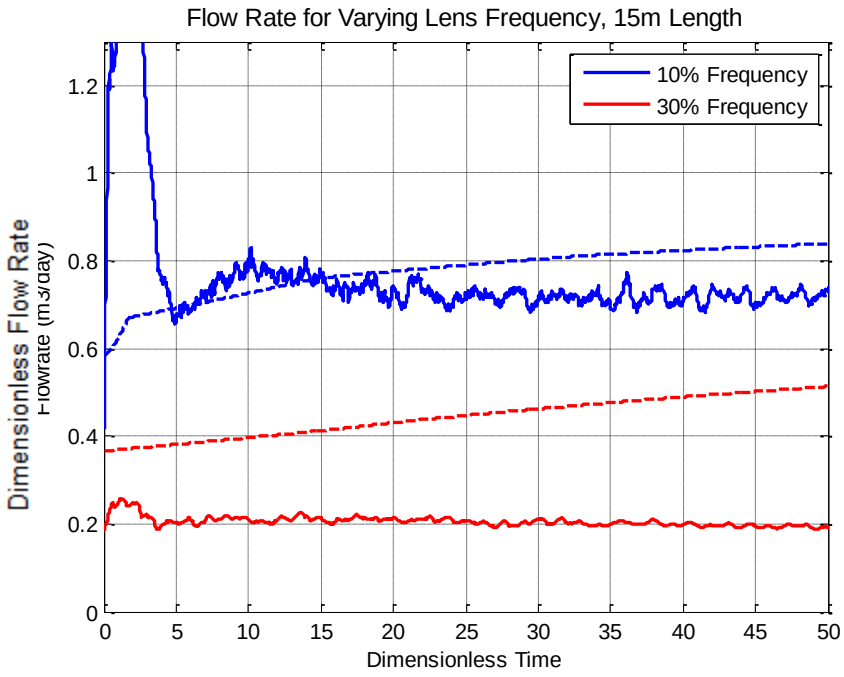

Figure 3.8: Dimensionless flow rate for varying lens frequency, 15m correlation length

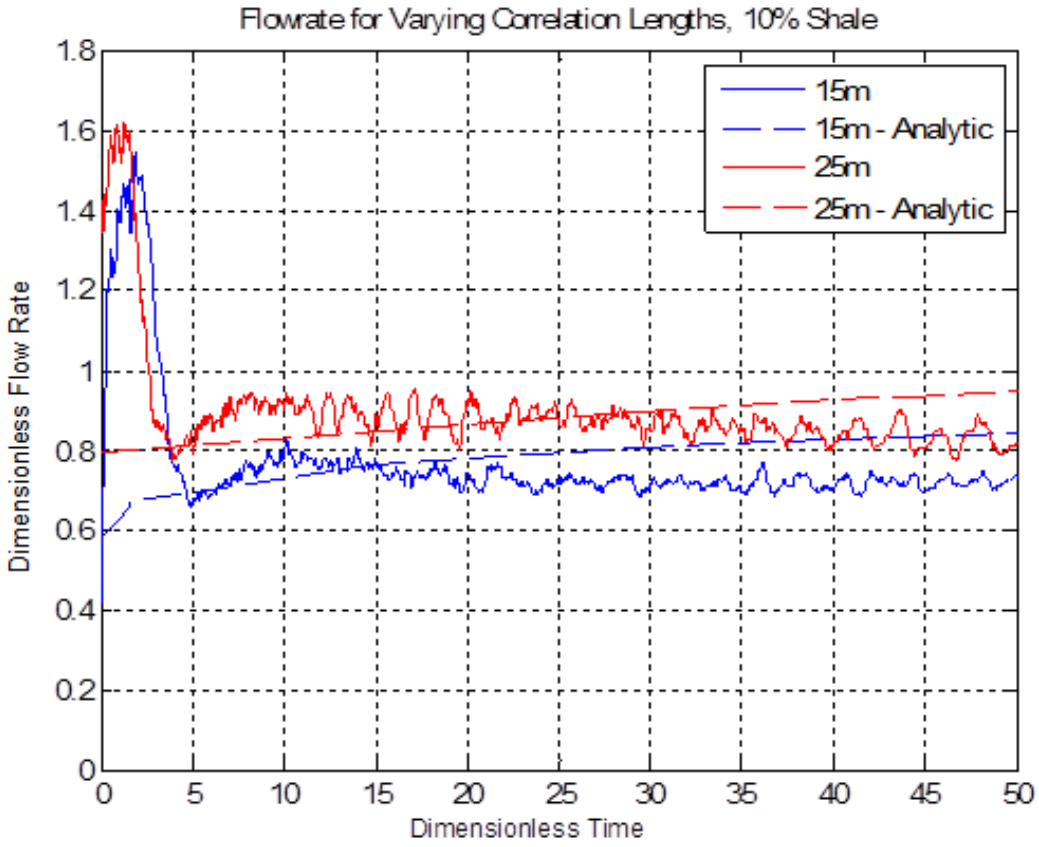

Figure 3.9: Dimensionless flow rate for varying lens lenses, 10% lens frequency

The anisotropic simulation flow rates obtained by varying the shale correlation length as well as the shale frequency result in dimensionless flow rates consistently lower than the analytic model result. The difference may be due to the fundamental assumption underlying Azom's model, the steam chamber grows in the shape of an ideal inverted triangle. Although the steam chamber growth in the simulation was triangular in shape, higher anisotropy cases favored a narrower width near the well pair and a wider shape close to the top of the reservoir layer. This created a larger half-width measurement compared to the ideal inverted triangle, resulting in the analytic model assuming more bitumen has been displaced than in reality. While the steam chamber width in the

simulation models is non-linear in time, the analytical model assumes a linear growth of the steam chamber in time.

Due to the inability of Azom's model to directly account for heterogeneity, it depends on the estimated values of effective directional permeability. Upscaling methods used to compute effective permeability have difficulty in capturing the separate impact of correlation length and lens frequency on the growth of the steam chamber. Therefore, a reservoir with high frequency and short correlation length may have identical effective permeability values as a reservoir with low frequency and long correlation length resulting in identical anisotropic and analytic flow rates. However, the steam chamber rise and spread in the heterogeneous model looks quite different for these cases as shown by Figures 3.10 and 3.11. These figures depict the time in the simulation when the steam chambers have risen to the top of the reservoir and begun to spread laterally.

Moreover, the upscaling scheme utilizes global boundary conditions that are inconsistent with the flow configuration encountered during the growth of the steam chamber. When the shale correlation lengths are shorter, the steam rise was only slightly interrupted as it moved around the barrier. The irregularities in steam chamber shape increased as the correlation length and frequency increased.

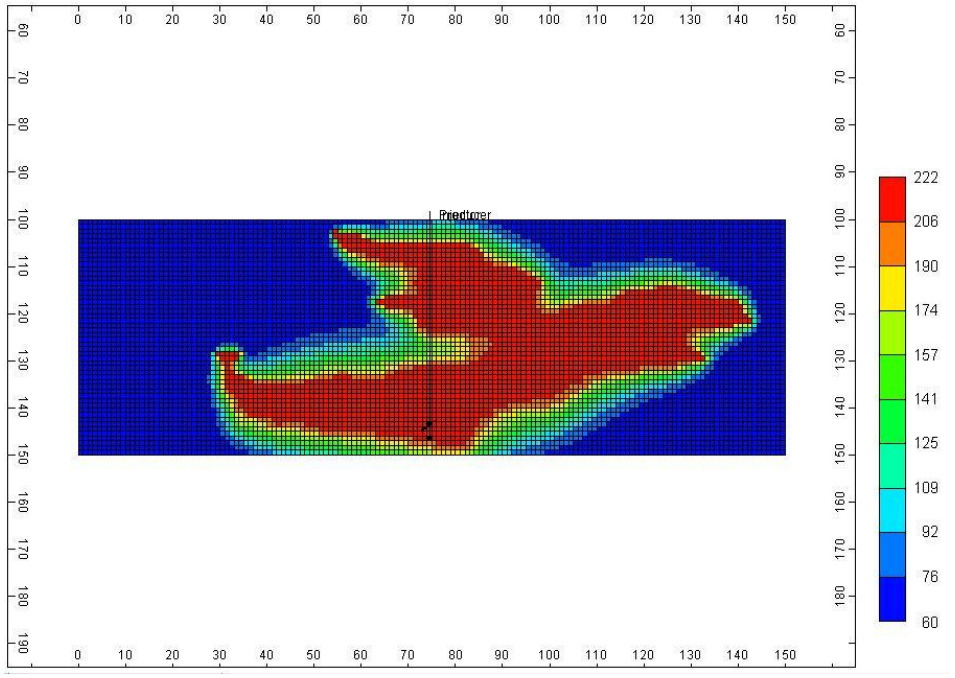

Figure 3.10: Steam Chamber for correlation length 25m, 10% Shale Proportion

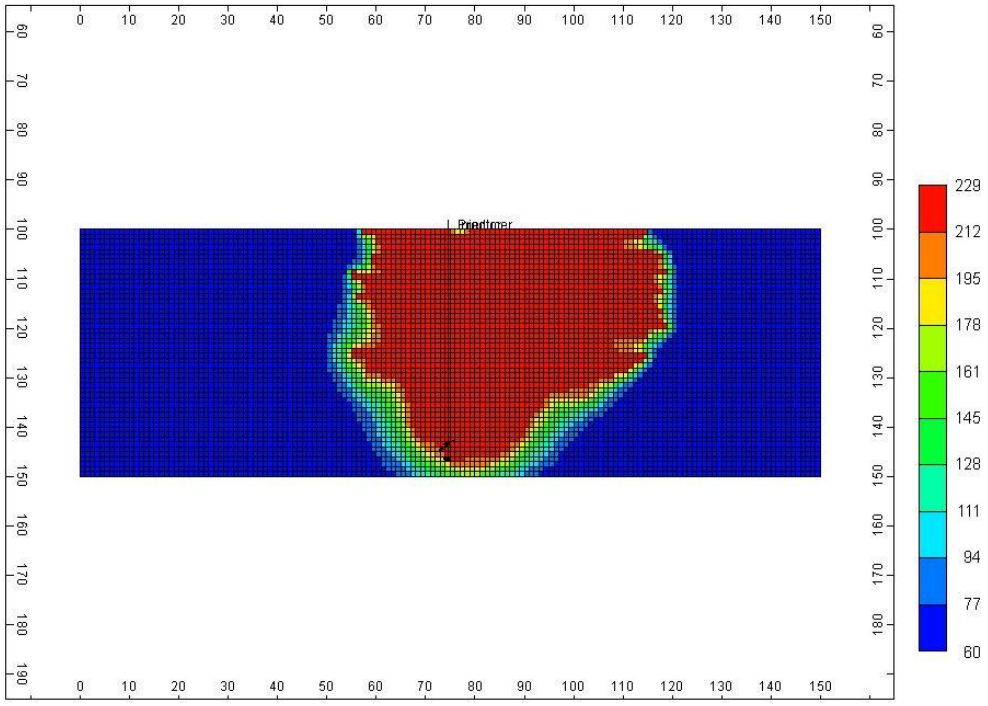

Figure 3.11: Steam Chamber growth for correlation length 5m, 50% shale proportion

It was determined that shale correlation length and lens frequency play a large role in the performance of the SAGD process. Increased correlation lengths and increased lens frequency both decrease the dimensionless flow rates at a given dimensionless time. Simulation results also suggest the importance of the steam chamber shape in the estimation of flow rates especially when compared to rates predicted by analytical models. Upscaling heterogeneous values for input into an analytic model, such as Azom's model, will result in an overestimation of flow rate due to the inability to fully account for the impact of reservoir barriers and the configuration of flow streamlines during the SAGD process.

While the Azom and Srinivasan model helped account for permeability anisotropy for certain cases with specified correlation length and shale proportion, the subsequent chapters will look at better ways to define effective anisotropic parameters that might help better predict the performance of the SAGD process using upscaled models.

Chapter 4: Modeling the Impact of Permeability Anisotropy on SAGD using a Statistical Upscaling Scheme

Thus far, all simulations and analysis have been conducted to validate analytical expressions for SAGD production that have been developed for the spread of a steam chamber in two-dimensional space. The effect of the correlation length of the shale streaks in the transverse direction is thus ignored. This chapter aims to determine relationships between fully heterogeneous models and equivalent anisotropic models in 3-dimensional space. Furthermore, we will attempt to model a statistical upscaling method such that the overall production profile for heterogeneous models is matched to the response from the corresponding anisotropic models.

4.1 STATISTICAL UPSCALING

Conventional physics-based upscaling techniques such as Durlofsky's method discussed in Chapter 3, make several assumptions regarding boundary conditions at the top of the reservoir, single phase fluid flow etc. that are inconsistent with the actual conditions during the SAGD process. In order to study these effects and to determine an effective relationship between fully heterogeneous and equivalent anisotropic models, a statistical procedure for calibrating effective anisotropic permeability values was developed.

Full 3-D, heterogeneous models were developed in SGeMS using the indicator simulation program SISIM (Remy et al. 2008). Simulating the mass and heat transfer processes associated with SAGD on a fully heterogeneous model such as the one shown

in Fig. 4.1 is computationally expensive, thus motivating the need for an equivalent anisotropic model to predict production rates.

Using statistical averaging techniques to estimate an effective permeability value for the entire reservoir is a common method practiced in the industry. Furthermore, Warren and Price (1961) first determined that using the geometric mean of individual permeability values in the entire reservoir is an effective way to estimate the overall reservoir heterogeneity. They believed that while all porous media are heterogeneous on the microscopic level, only macroscopic fluctuations need consideration since reservoir mechanics are based on macroscopic quantities. Jensen (1991) stated that the use of geometric averaging to calculate the effective permeability is appropriate under certain conditions. Matheron (1967), Bakr et al. (1978), Gutjahr et al. (1978) and Dagan (1979, 1981) also studied this and found that geometrically averaging can be effective when permeabilities are log-normally distributed with low variance. However, none of these studies attempted to determine statistical relationships between the averaged effective permeability to the production response. We aim to further these studies by using statistical averaging techniques to model the production response for heterogeneous reservoirs.

The statistical method is tested on two models exhibiting distinctly different correlation lengths of discontinuous shale lenses: 25m x 5m x 5m and 50m x 10m x 10m in the x, y, and z directions respectively. These shale lenses are stochastically distributed in a reservoir with grid dimensions of 25x80x35 in the x, y, and z directions, respectively. The dimension for each cell in the grid is 20m x 2m x 1m in the x, y, and z directions,

respectively. The reservoir properties are kept the same as previous cases outlined in Chapter 3.

Effective permeability values were calculated for full 3D heterogeneous reservoirs using three different statistical averaging techniques shown in Table 4.1. Using these values as initial guesses for the upscaled permeability, k_v and k_h were optimized individually. This was done to provide more flexibility to the regression process and to evaluate the influence of each variable separately. Additionally, k_v and k_h may in some cases have competing influence on the oil recovery and consequently, optimizing the ratio k_v/k_hmay in such cases be sub-optimal.

4.2 UPSCALING APPROACH

As mentioned earlier, the values of k_v and k_h obtained from the statistical upscaling methods are used as the initial guess in an iterative procedure to determine the optimal k_v and k_h necessary to match the production profile of the fully heterogeneous model.

4.2.1 Initial Guesses

Fig. 4.2 compares the initial guesses corresponding to the three different statistical upscaling methods tested for one specific heterogeneous case with a specific set of shale parameters i.e. correlation length and shale proportion. To begin the statistical upscaling process, the entire heterogeneous reservoir grid was discretized into individual cell blocks containing permeability values in each spatial direction. We had initially planned to run simulations on a grid with dimensions of 250x160x35 with cell dimensions 2m x 1m x 1m. However, such a fine scale grid would be computationally inefficient and would be

difficult to compare to anisotropic cases in a timely manner. Therefore, the above grid was upscaled to a coarser grid with dimensions 25x80x35 with cell dimensions 20m x 2m x 1m using Durlofsky's method to optimize on computation time. In doing so a new set of discretized permeability values were generated for the reservoir grid. The discretized values were sorted according to their spatial orientation in an array and the different statistical upscaling schemes shown in Table 4.1 were utilized to determine an effective permeability value for the anisotropic model. Flow simulation was performed using the upscaled permeability values and the results were compared to the heterogeneous model response.

It was concluded that performing upscaling using geometric averaging produced the best initial match to the fully heterogeneous model. Therefore, subsequent analysis will be based on the geometric upscaling technique. Because harmonic averaging is overly influenced by lower values such as shale permeability, it produced extremely poor matches to the heterogeneous response.

Table 4.1: Different Statistical Upscaling Methods

Statistical Upscaling Technique	Function
Arithmetic	$k_{avg-eff} = \frac{1}{n}\sum_{i=1}^{n} k_i$
Geometric	$k_{geo-eff} = \sqrt[n]{\prod_{i=1}^{n} k_i}$
Harmonic	$k_{har-eff} = \frac{1}{\frac{1}{n}\sum_{i=1}^{n}\frac{1}{k_i}}$

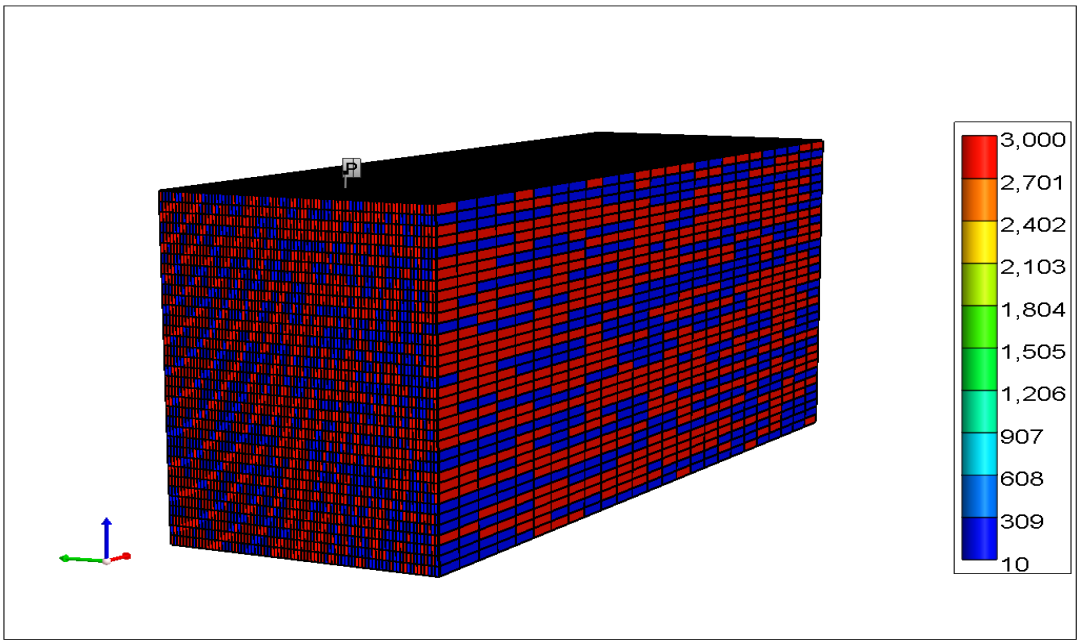

Figure 4.1**:** An example of a fully heterogeneous model

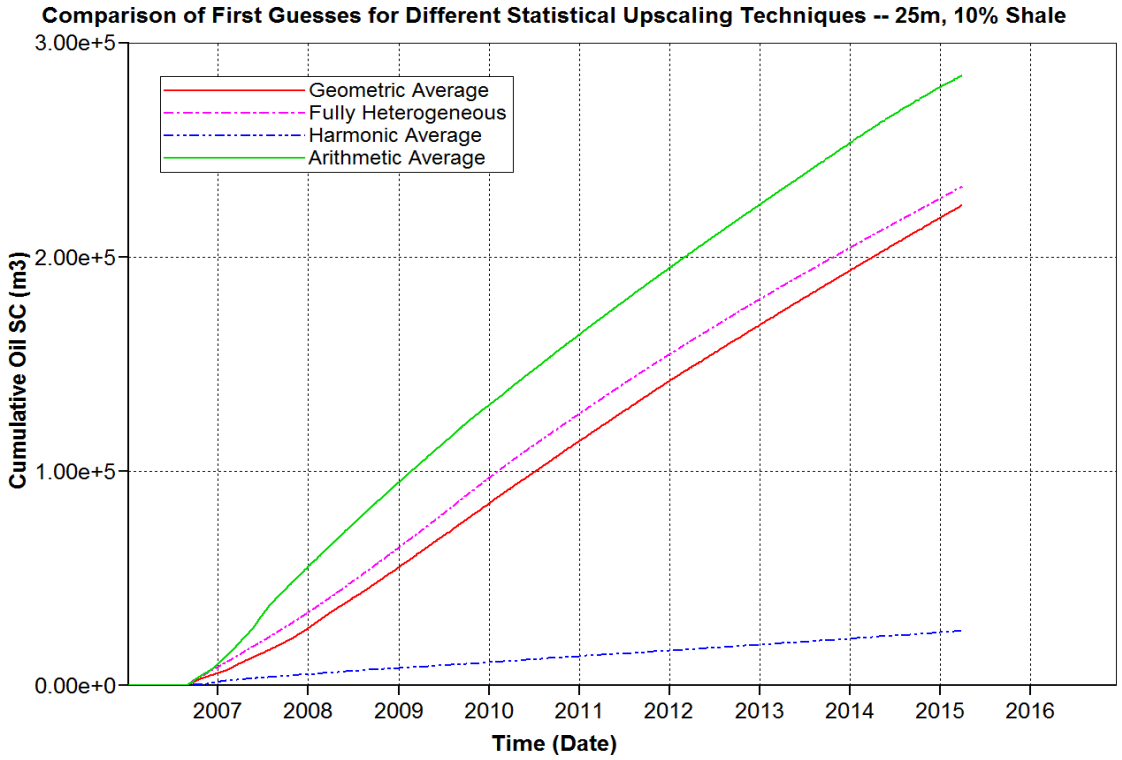

Figure 4.2: Cumulative Oil Output for the Heterogeneous model compared to that using upscaled permeability values.

4.2.1 Optimization of K_V

Starting with the initial guess value, k_v is iteratively changed while keeping k_h constant. After four such guesses, non-linear regression is performed using the changed k_v values and the corresponding cumulative recovery. A 2nd order polynomial expression is fit to represent the relationship between k_v and cumulative oil recovered. This fitted polynomial equation is used (in lieu of full physics flow simulation) to optimize the value of k_v. The Generalized Reduced Gradient (GRG2) algorithm is used to compute the optimal value of the effective permeability. GRG2 is an effective algorithm for solving nonlinear optimization problems and is widely used in the Solver function found in

Microsoft Excel (Lasdon and Waren 1981). The anisotropic permeability values calculated by the GRG2 algorithm is then tested in the simulator and compared with the cumulative oil recovered in the fully heterogeneous model. This process is then repeated to determine an optimal k_h so that the updated relationship between k_v/k_h and cumulative oil recovered can be generated. Other regression techniques such as logarithmic regression and exponential regression did not yield satisfactory matches to the fully heterogeneous model.

As mentioned earlier, k_v is iteratively changed while k_h is kept constant After making four guesses for an optimal k_v ratio, polynomial regression was performed on the relationship between cumulative oil and the effective k_v. The quality of the regression improves with more number of initial guesses, but for all cases presented a minimum of 4 guesses were used to optimize on the computational time. Generally, one guess of k_v was made such that it would yield an overestimate of the volume of oil recovered in the parent heterogeneous model, one guess yielded an underestimate, and one guess in the middle of the range of k_v value expected. The 4th guess was an initial assumption that when $k_v = 0$, the volume of oil recovered was negligible ~ 0.

The GRG2 algorithm was then utilized using the polynomial expression and an optimal k_v was determined such that the cumulative oil output was a close match to the cumulative oil output generated by the corresponding fully heterogeneous model. The iterative optimization procedure is shown in Fig. 4.3 and tabulated in Table 4.2. To validate whether this k_v value was optimal, that value was input into the simulator and

the resultant flow simulation result was compared to the fully heterogeneous model, as shown in Fig. 4.4.

For the case shown in Fig. 4.4, cumulative oil recovery obtained by specifying $k_v = 97.19mD$ is 30382m^3. The original heterogeneous cumulative oil output was found to be 30469m^3, and therefore the error in prediction is less than 1%. The heterogeneous model corresponded to a case with shale correlation length, L = 25m and high shale proportion, SP = 50%. Table 4.3 shows the final k_v necessary to match the fully heterogeneous system for all different cases that were tested. Each case in Table 4.3 is an average of 5 different realizations simulated. In all these cases, the horizontal permeability was calculated using a geometric average.

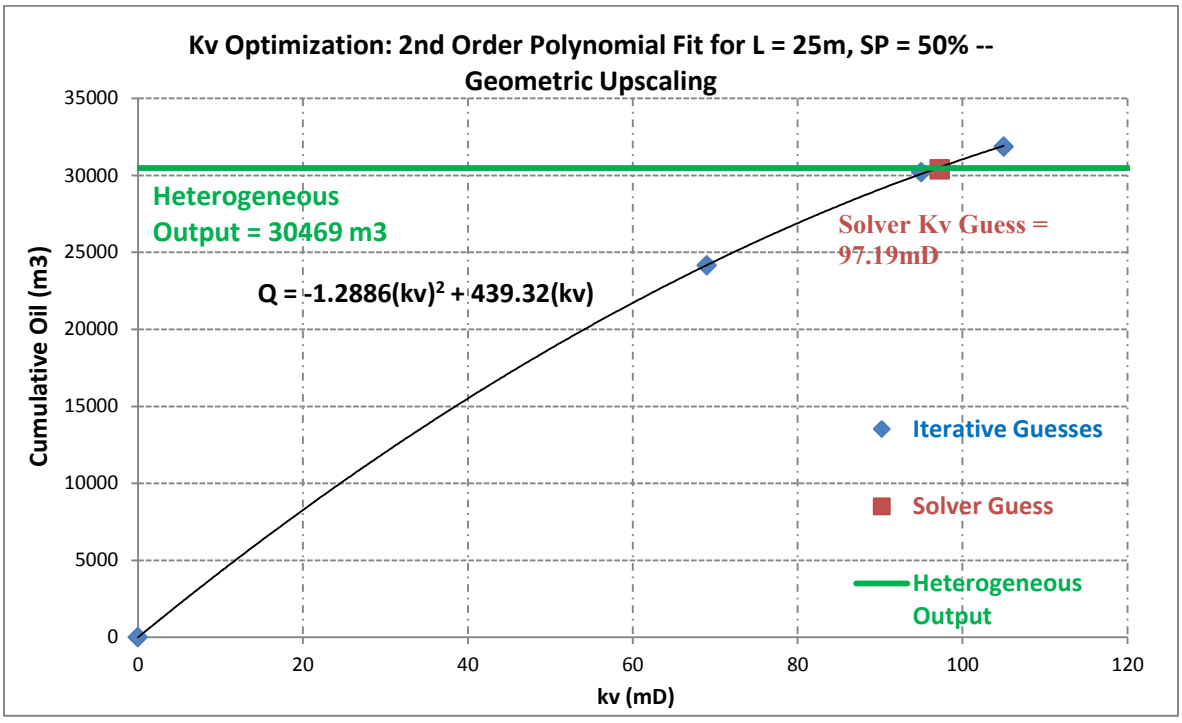

Figure 4.3: K_V optimization using polynomial regression performed on case with a shale correlation length of25m and a shale proportion of 50%

Table 4.2: Iterative Guesses and Solver Match to Heterogeneous Model corresponding to shale correlation length of 25m and proportion of 50%

Initial k_h = 521.43, Heterogeneous Output = 30469m3				
Guess #	k_v (mD)	k_v/k_h	CMG Cumulative Oil (m3)	% Error
Assumption	0	0	0	-
1	69	0.133	24142	20.77
2	95	0.182	30204	0.87
3	105	0.201	31860	4.57
Solver Guess	*97.19*	*0.186*	*30382*	*0.29*

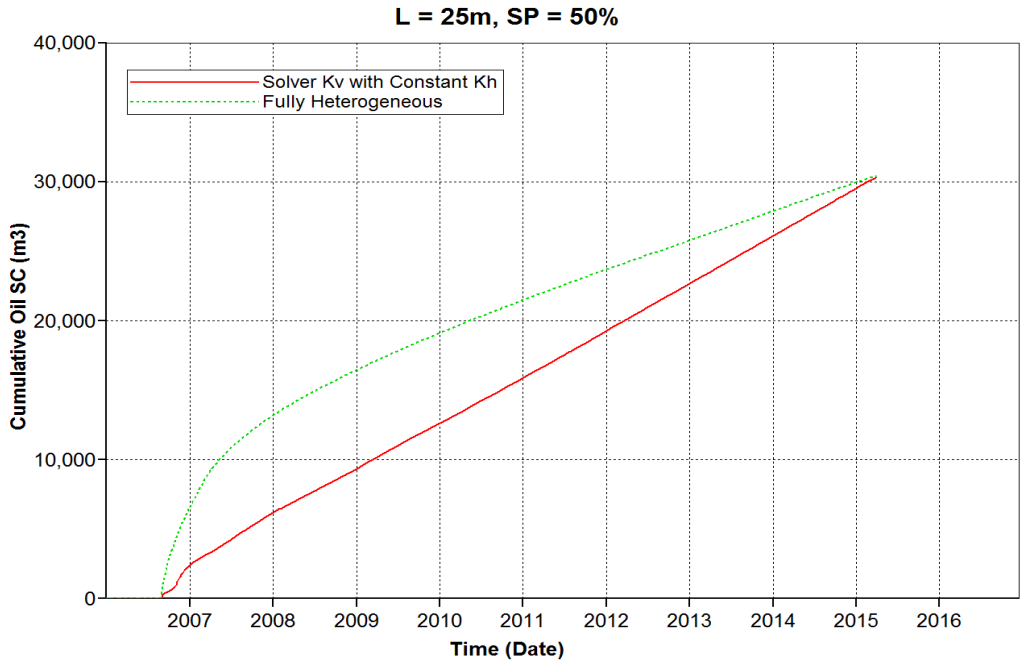

Figure 4.4: Comparison of the response using the optimized: K_V value and that corresponding to the heterogeneous model with shale correlation length of 25m and proportion of 50%

Table 4.3: K_V optimized to match heterogeneous output. The comparison is the average over 5 realizations.

Correlation Length (m)	Shale Proportion (%)	Heterogeneous Cumulative Oil Output (m3)	Initial k_v (mD) Guess	Optimal k_v (mD) via Solver	Constant k_h (mD) from initial guess	Cumulative Oil (m3) using Solver k_v	Error (%)
25	50%	30,485	69	99	523	29,950	1.7
25	30%	62,810	223	202	1,245	62,799	~ 0
25	10%	232,850	1,029	1,178	2,288	232,451	~ 0
50	50%	35,205	107	158	335	32,330	0.53
50	30%	81,573	346	355	902	80,251	1.62
50	10%	248,659	1,273	1,625	1,998	253,204	1.83

4.2.2 Optimization of K_H

The same procedure used to optimize k_v was used to optimize k_h with the exception of keeping the optimized k_v constant. This would help determine the overall impact of k_v and k_h and give us a little bit more flexibility to match the heterogeneous response. The regression analysis for k_h including the iterative guessing procedure is shown in Fig. 4.5 and tabulated in Table 4.4. The initial guess corresponded to the value computed using the geometric average. The analysis shown in these figures are for the same case with the shale correlation length of 25m and shale proportion of 50%. The optimized value of k_h was then specified as an input into the simulator and the accuracy of the new anisotropic model was compared.

The process of optimizing k_h, further improved the overall match to the heterogeneous model response. Since the initial optimization of k_v was already very

accurate, many optimized k_h values were relatively close to their initial guess. Furthermore, during the optimization process, it was observed that the impact of k_h on production wasn't nearly as significant as the impact of k_v.

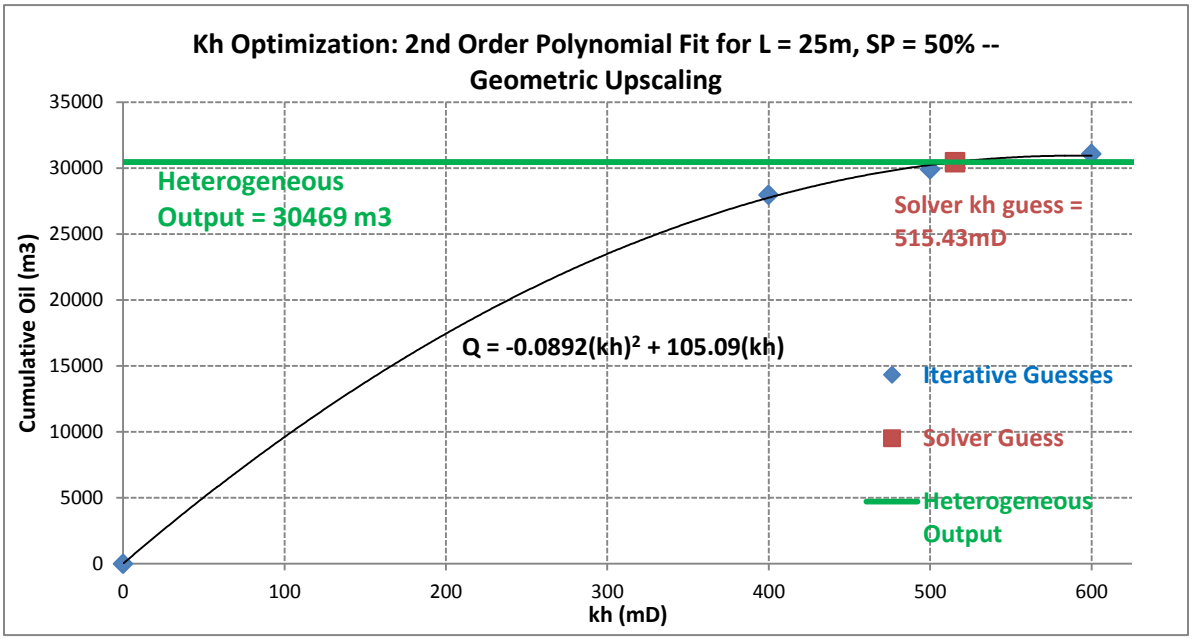

Figure 4.5: K_H optimization using polynomial regression for the case with shale correlation length of 25m and shale proportion of 50%

Table 4.4: Iterative Guesses and Solver Match for K_H to minimize the deviation from the heterogeneous model response corresponding to a shale correlation length of 25m and a shale proportion of 50%.

Optimized k_v = 97.19mD, Heterogeneous Output = 30469m3				
Guess #	k_h (mD)	k_v/k_h	CMG Cumulative Oil (m3)	% Error
Assumption	0	~ 0	0	-
1	400	0.243	27970	8.20
2	500	0.194	29910	1.83
3	600	0.162	31077	2.00
Solver Guess	*515.44*	*0.189*	*30465*	*0.01*

Specifying the optimized value of $k_h = 515.44mD$ and the previously optimized value of $k_v = 97.19mD$ into the simulator, the recovered oil was found to be 30465m^3 which was nearly exactly as much produced by the fully heterogeneous model (30469m^3). This match is shown in Fig. 4.6. Similar analysis was performed for all cases of shale correlation length and the optimal k_h and k_v values are shown for each case, in Table 4.5. The values shown in this table are the average of 5 realizations for each case.

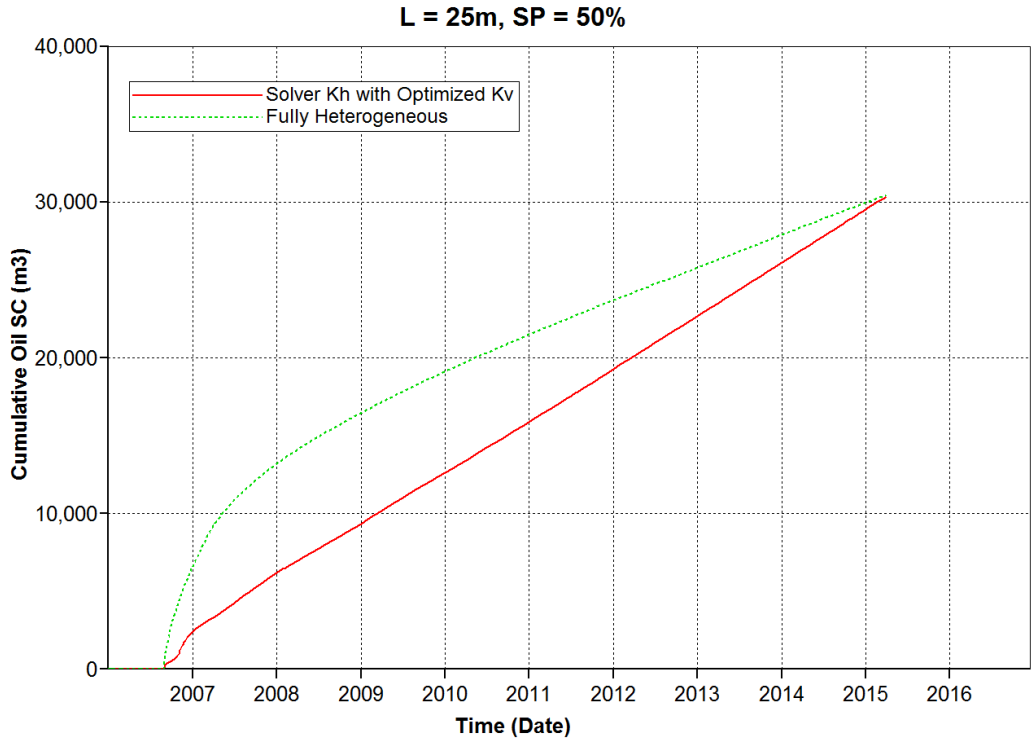

Figure 4.6: K_H determined via solver to match case with L = 25m, SP = 50%

Table 4.5: Optimized K_H to match Heterogeneous Output – Geometric Upscaling (Average of 5 realizations)

Correlation Length (m)	Shale Proportion (%)	Heterogeneous Cumulative Oil Output (m3)	Initial k_h (mD) Guess	Optimal k_h (mD) via Solver	Optimized k_v (mD) kept constant	Cumulative Oil (m3) using Solver k_v/k_h	Error (%)
25	50%	30,485	523	516	99	30,450	~ 0
25	30%	62,810	1,245	1,210	202	62,799	~ 0
25	10%	232,850	2,288	2,150	1,178	232,451	~ 0
50	50%	35,205	335	305	158	35,130	~ 0
50	30%	81,573	902	850	355	81,450	~ 0
50	10%	248,659	1,998	2,300	1,625	249,650	~ 0

With the error in prediction nearly zero for each case, we can perform analysis on the k_v/k_h ratio. Additionally, based on these improved results, we can perform multi-variable regression on the relationship between the correlation length, shale proportion and k_v/k_h. Chapter 5 will demonstrate the ability to calibrate such a relationship and determine the necessary k_v/k_h that corresponds to a given correlation length and shale proportion.

Chapter 5: Regression Analysis to Determine Relationship between Shale Properties and Permeability Anisotropy affecting SAGD Performance

Chapter 4 presented an optimization procedure for calculating anisotropic permeability values, k_v and k_h such that the corresponding production response of the SAGD process would match that for parent heterogeneous model using which the upscaled values were computed. We had shown in Table 4.6 that there exists a non-unique relationship between k_v/k_h and cumulative oil recovered. To better constrain the relationship between k_v/k_h and oil recovery, we attempted to develop a relationship between shale correlation length, proportion and k_v/k_h. To do so, we must perform multi-variable regression using these variables and test the effectiveness of using such a regression to accurately predict reservoir performance.

5.1 MULTI-VARIABLE REGRESSION

In Chapter 4 we took several realizations of the heterogeneous models with varying shale proportion and correlation length and established the corresponding optimal k_v and k_h values that matched the oil recovery of the heterogeneous models. The optimization procedure required initial guesses for the anisotropic permeability - $k_{v,initial}$, and $k_{h,initial}$. A regression surface was fitted using the initial guesses and some other values of k_v and $k_h$and the corresponding volume of oil recovered and this regression surface was used to converge to the optimal values for the parameters. The Curve Fitting Toolbox in MATLAB was used extensively to determine the regression surfaces and optimization was performed using the iterative procedure discussed in Chapter 4.

5.1.1 Regression surface using optimized K_V values

To compare the effect of optimizing k_v and k_h separately, multi-variable regression was performed using the optimized k_v values while keeping the k_h equal to the initial guess for the cases in Chapter 4. The corresponding k_v/k_h was plotted against the shale correlation length λ and shale proportion (SP) in order to generate a surface that would allow for interpolation. Figure 5.1 shows the relationship between these variables while Table 5.1 displays the expression that was used to model the surface. The expression generated was of 1st order in shale correlation length λ, and 2nd order in shale proportion, SP. Many other polynomial forms were attempted but the expression in Table 5.1 was the final form that yielded an acceptable surface that minimized the deviation from the observed heterogeneous response. The calibration implies a strong non-linear relationship between shale proportion and the anisotropy ratio k_v/k_h. The sensitivity to shale correlation length is somewhat lower, however the combination of the two shale parameters significantly influence the optimal k_v/k_h values.

We calibrated a similar relationship between the initial guess values for k_h for the above cases and the shale characteristics. The surface that fits the relationship between λ, SP, and k_h is shown by Figure 5.2 while the expression that models the surface is shown in Table 5.2.

Given a set of parameters describing the spatial distribution of shales in the reservoir, the k_v/k_h value can be retrieved from the surface in Figure 5.1. The value of k_h can be retrieved from Figure 5.2 and consequently the value of k_v can be calculated.

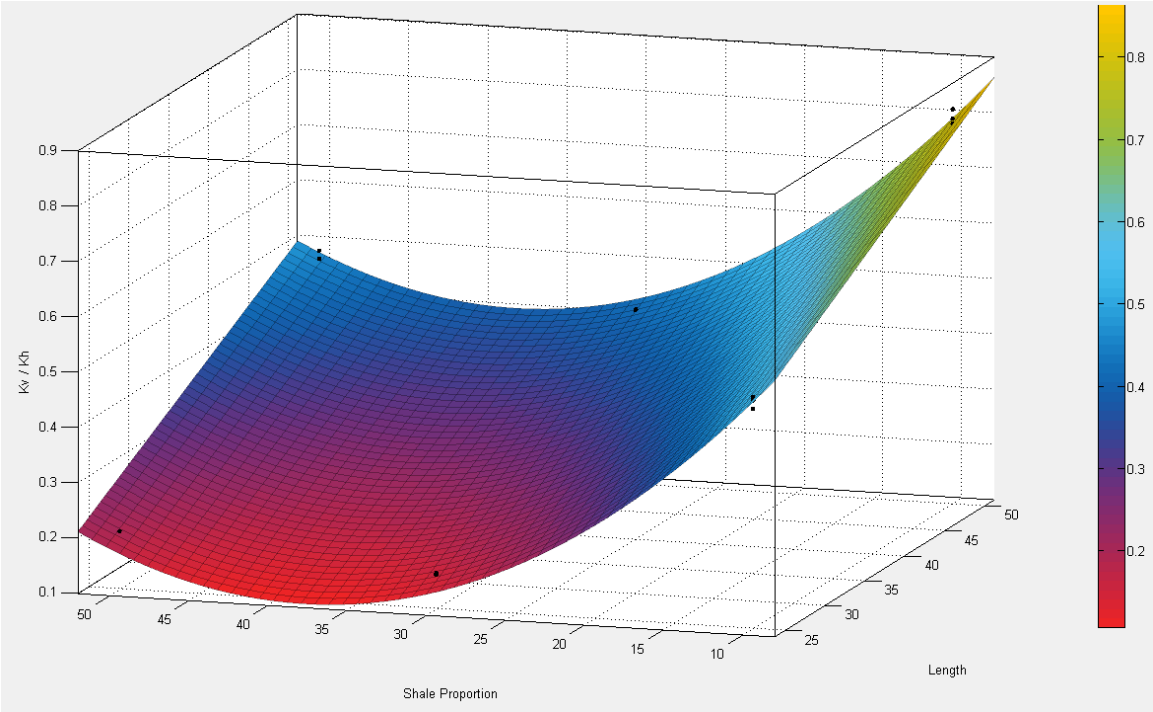

Figure 5.1: Regression surface describing the relationship between shale correlation length, shale proportion and K_V/K_H value

Table 5.1: Coefficients of the regression surface relating λ, SP to K_V/K_H

Expression Format: $\frac{k_{v,optimal}}{k_{h,initial}} = p_{00} + \lambda * p_{10} + SP * p_{01} + \lambda * SP * p_{11} + SP^2 * p_{02}$				
p_{00}	p_{10}	p_{01}	p_{11}	p_{02}
0.5986	0.01131	-0.04068	-1.643e-05	0.0005489

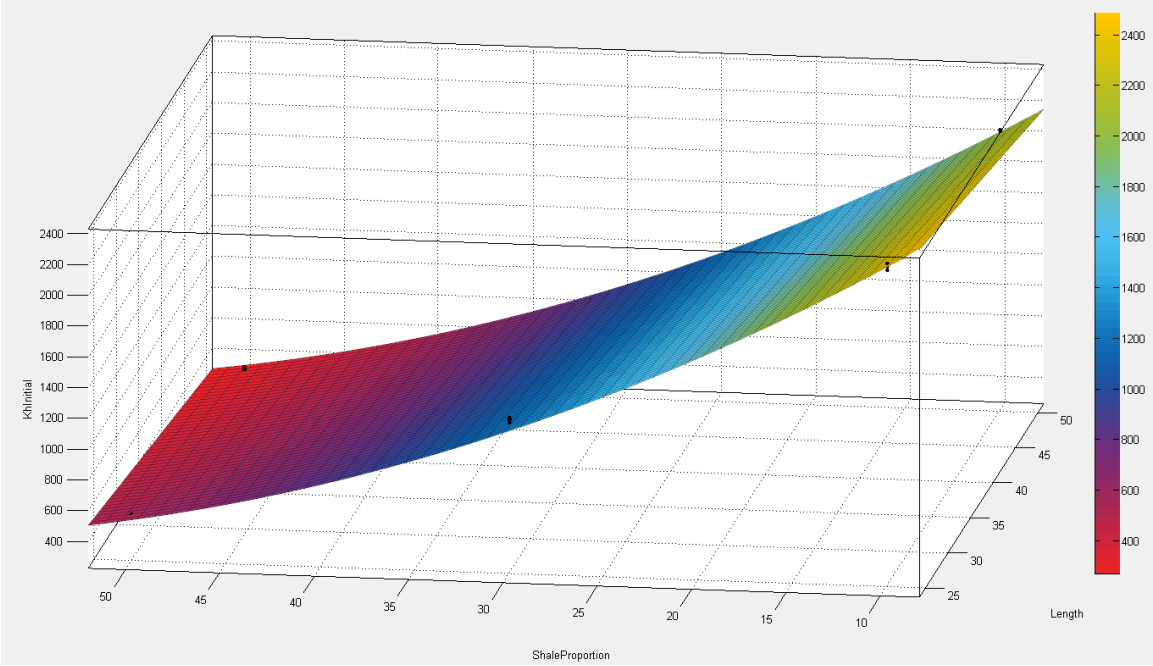

Figure 5.2: Regression surface relating λ, SP, to K_H

Table 5.2: Coefficients of the regression relating λ, SP to K_H

Expression Format: $k_{h,initial} = p_{00} + \lambda * p_{10} + SP * p_{01} + \lambda * SP * p_{11} + SP^2 * p_{02}$				
p_{00}	p_{10}	p_{01}	p_{11}	p_{02}
3415	-13.31	-83.45	0.08876	0.6065

5.1.2 Regression surface using optimized K_V and K_H values and

We saw in Table 4.6 that there was a difference in the value for $\frac{k_v}{k_h}$ when both k_v and k_h values are optimized, In order to investigate the relationship between the shale properties and the optimized value for $\frac{k_v}{k_h}$ in this case, the multivariable regression

procedure was repeated. The same process as before was employed to regress a surface to fit λ, SP, and $\frac{k_v}{k_h}$ in this case. Figure 5.3 displays the fitted surface while Table 5.3 displays the coefficients defining the surface. It can be observed that even though the difference in magnitude between the $\frac{k_v}{k_h}$ values in Figures 5.1 and 5.3 is very little, the fitted surfaces look substantially different. The surface describing the relation between k_h, λ and SP is shown by Figure 5.4 with the corresponding coefficients summarized in Table 5.4.

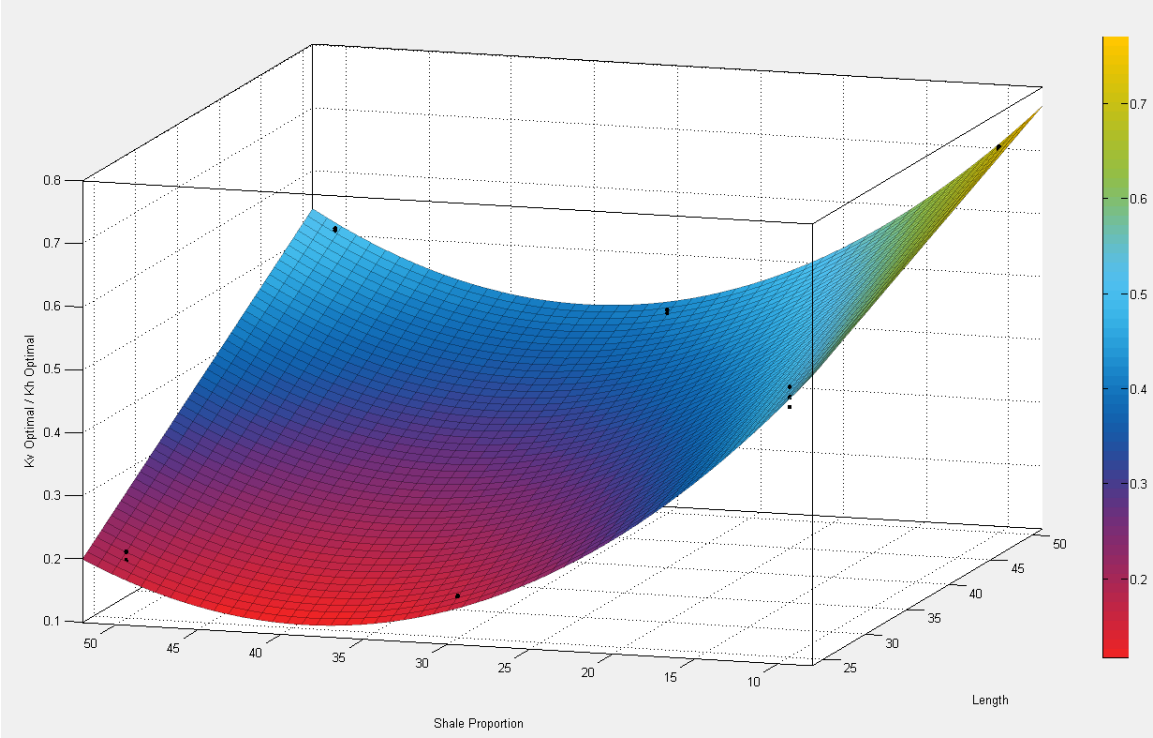

Figure 5.3: Regression surface fitting Length, Shale Proportion to $K_{V\_Optimal}/K_{H\_Optimal}$

Table 5.3: Coefficients of the regression surface relating λ, SP to K_V/K_H

Expression Format: $\frac{k_{v,optimal}}{k_{h,optimal}} = p_{00} + \lambda * p_{10} + SP * p_{01} + \lambda * SP * p_{11} + SP^2 * p_{02}$				
p_{00}	p_{10}	p_{01}	p_{11}	p_{02}
0.7639	0.004801	-0.0429	0.000167	0.0004971

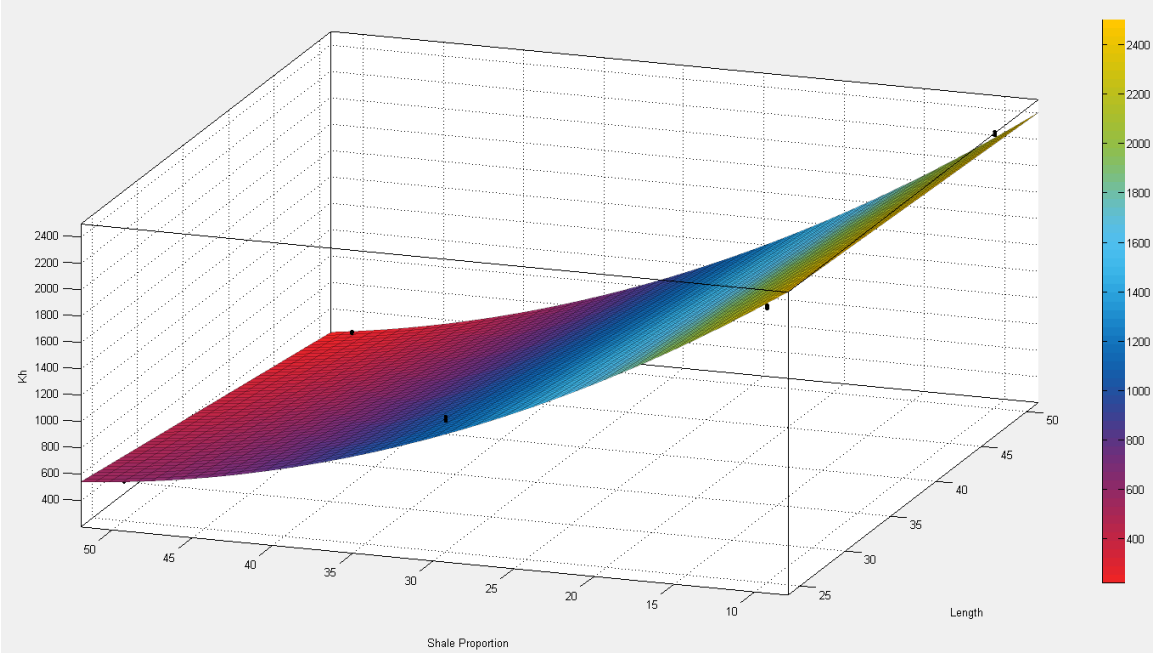

Figure 5.4: Regression surface fitting Length, Shale Proportion to K_H

Table 5.4: Coefficients of the regression surface relating λ and SP to K_H

Expression Format: $k_{h,optimal} = p_{00} + \lambda * p_{10} + SP * p_{01} + \lambda * SP * p_{11} + SP^2 * p_{02}$				
p_{00}	p_{10}	p_{01}	p_{11}	p_{02}
3248	-2.774	-86.48	-0.1543	0.7584

Because the regression expression obtained when only the k_v is optimized is quite different from that obtained when both k_v and k_h are jointly optimized, it is clear that the same set of shale parameters would yield quite different values for the $\frac{k_v}{k_h}$ ratio. Table 5.5 outlines the difference in expressions based on the different optimizing procedures. If a point was chosen at random on the surface with coordinates λ = 47.81m and SP = 43.2%, each expression would yield different values for $\frac{k_v}{k_h}$ ratio and for k_h, as summarized in Table 5.5. It was observed in Chapter 4 that jointly optimized k_h and k_v yielded closer matches to the oil recovery profile for the parent heterogeneous models, and so the regression surfaces in Figures 5.3 and 5.4 will be used for further validation.

Table 5.5: Comparison of modeling expressions for K_V/K_H and K_H, when i) only K_V is optimized, ii) when both K_V and K_H are optimized. The computed values for K_V/K_H and kh using both expressions for a typical set of shale parameters is also shown.

Expression Format: $Z = p_{00} + \lambda * p_{10} + SP * p_{01} + \lambda * SP * p_{11} + SP^2 * p_{02}$						
Z	p_{00}	p_{10}	p_{01}	p_{11}	p_{02}	When λ = 47.81m, SP = 43.2%
$\frac{k_v}{k_h}\|Fig.5.1$	0.5986	0.01131	-0.04068	-1.643e^{-05}	0.0005489	0.370
$\frac{k_v}{k_h}\|Fig.5.3$	0.6573	0.006841	-0.03882	0.0001051	0.0004695	0.401
$k_h\|Fig.5.2$	3415	-13.31	-83.45	0.08876	0.6065	489.2
$k_h\|Fig.5.4$	3248	-2.774	-86.48	-0.1543	0.7584	448.3

5.2 VALIDATION OF MULTI-VARIABLE REGRESSION

Three points were chosen at random from the fitted regression surfaces in Figures 5.3 and 5.4 in order to check if the resultant anisotropy parameters yielded close match to the corresponding heterogeneous model responses. The chosen points were meant to cover various different parts of the surface to check for the global optimality of the model and are shown in Table 5.6. For a visual representation of where these points lie on the regression surface, please see Figure 5.5.

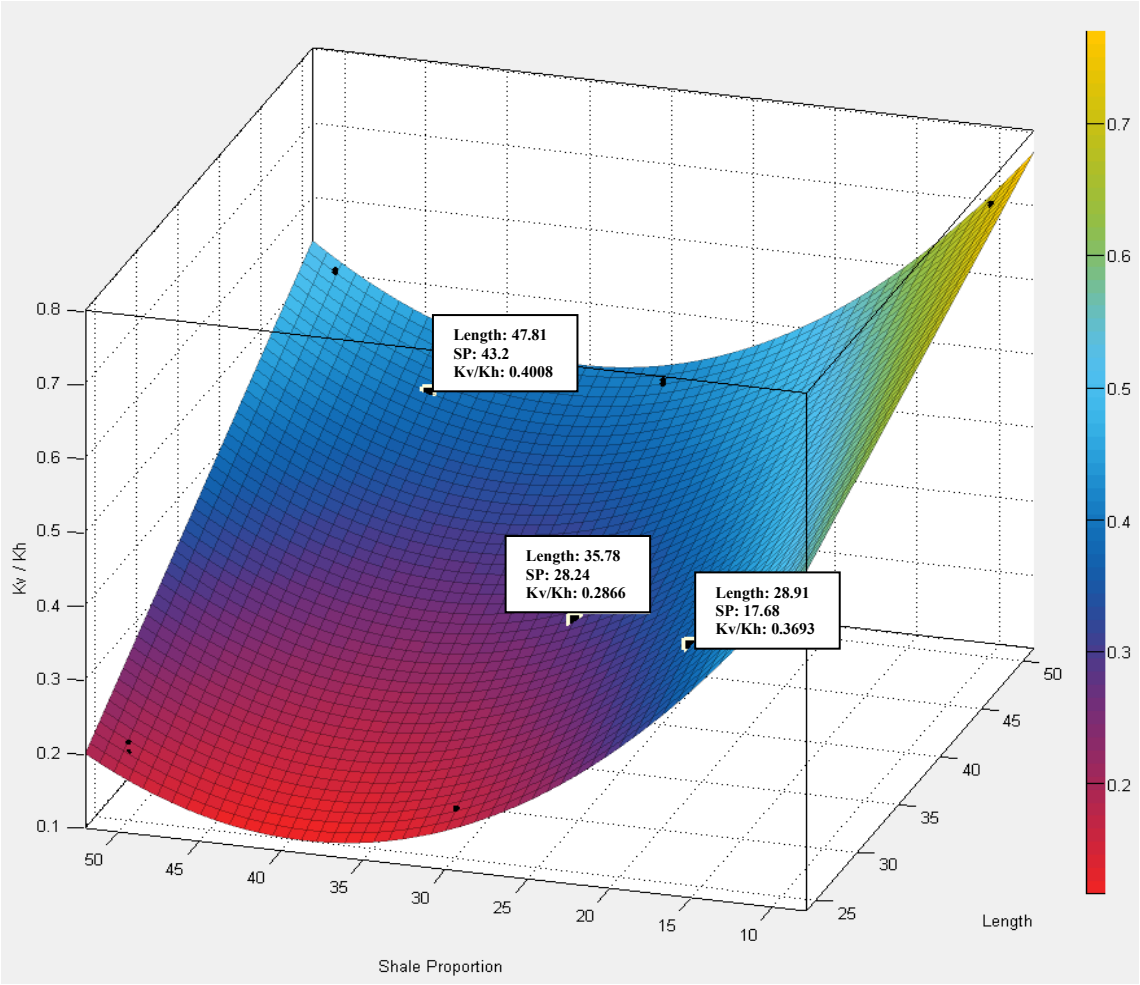

Figure 5.5: Points chosen on surface for validation

Table 5.6: Parameter values chosen for the validation cases.

Point	Length (m)	Shale Proportion (%)	$\frac{k_v}{k_h}$	k_h (mD)
1	28.91	17.68	0.3693	1783
2	35.78	28.24	0.2866	1135
3	47.81	43.2	0.4008	448.3

5.2.1 Validating Initial 3D Model

Heterogeneous sand-shale models corresponding to the specifications outlined in Table 5.6 were created using SGeMS. The correlation lengths and shale proportions were input to the sisim (Deutsch and Journel, 1998) algorithm. The SAGD process was simulated using the generated reservoir models in order to obtain the reference responses. The k_v/k_h and corresponding k_h shown in Table 5.5 were used for the anisotropic simulations. Table 5.7 summarizes the response of the heterogeneous model, the parameters for the anisotropic model obtained from Figure 5.5 corresponding to the chosen set of shale parameters. Specifying these permeability values into the flow simulator yielded the production response curves shown in Figures 5.6, 5.7, and 5.8. These are compared to the response curves from the parent heterogeneous model shown.

Table 5.7: Optimal K_V and K_H values from 3D model

Point	Length (m)	Shale Prop. (%)	Heterogeneous Model Cumulative Oil Output (m3)	$\frac{k_v}{k_h}$ (from Fig. 5.5)	k_h (mD) (from Fig. 5.5)	k_v (mD)
1	28.91	17.68	217071	0.369	1783	663.5
2	35.78	28.24	124201	0.286	1135	330.9
3	47.81	43.2	41324	0.401	448.3	190.7

It can be observed that only point 3 with λ = 47.81m, SP = 43.2 was a good match to the corresponding heterogeneous model response. This inaccuracy of the response obtained using equivalent anisotropic parameters is expected because the regression

surface was based only on a few combination of shale parameters sampling the outer limits of the surface, i.e. 25m and 50m with 10-30% shale proportion. In fact, the third parameter set yielded a good estimate simply because it closely resembled one of the models used for calibrating the regression surface.

Because regression is generally improved by having more representative data, the procedure was repeated with more data somewhere in between the cases used earlier. In order to generate a more accurate prediction model, the 3 points were optimized like the other cases using the iterative method discussed in Chapter 4 and the new k_v and k_h required to match he heterogeneous model response is shown in Table 5.8. Once determined, these additional data points will be used to establish a new regression surface. This will allow the prediction of the oil recovered from the anisotropic model to more closely match the corresponding heterogeneous model response.

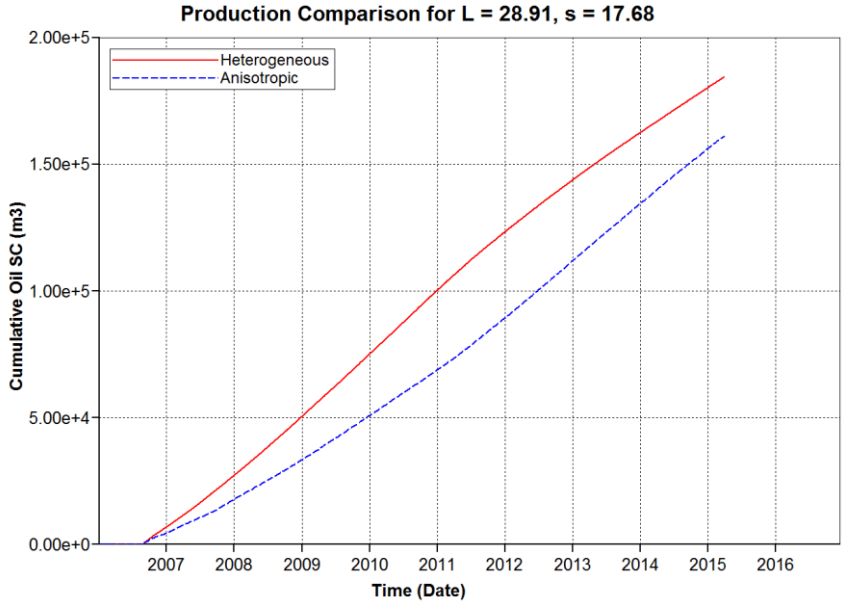

Figure 5.6: Heterogeneous vs. Anisotropic production response for model with λ = 28.91m, SP = 17.68%

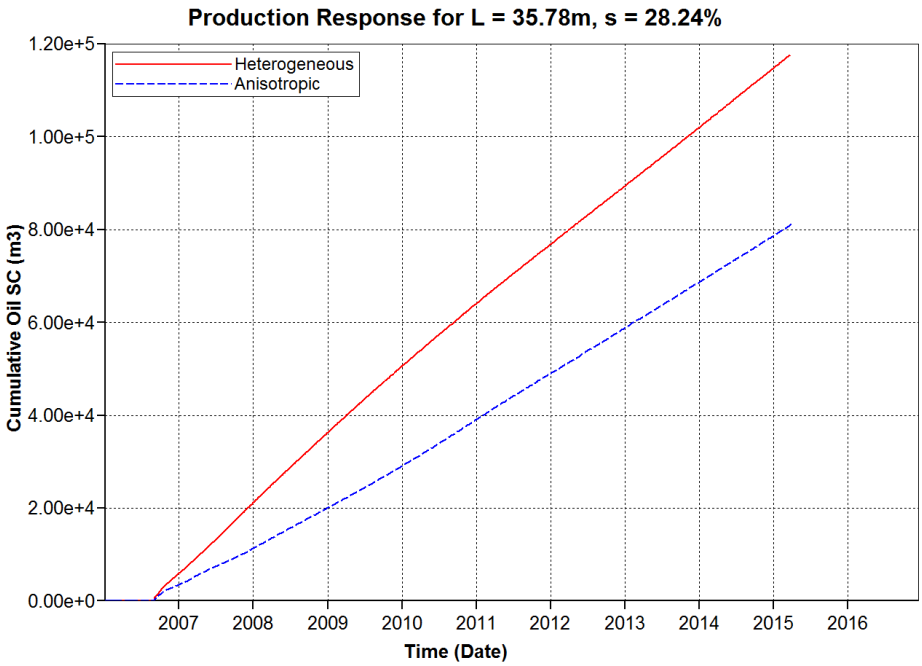

Figure 5.7: Heterogeneous vs. Anisotropic production response for λ = 35.78m, SP = 28.24%

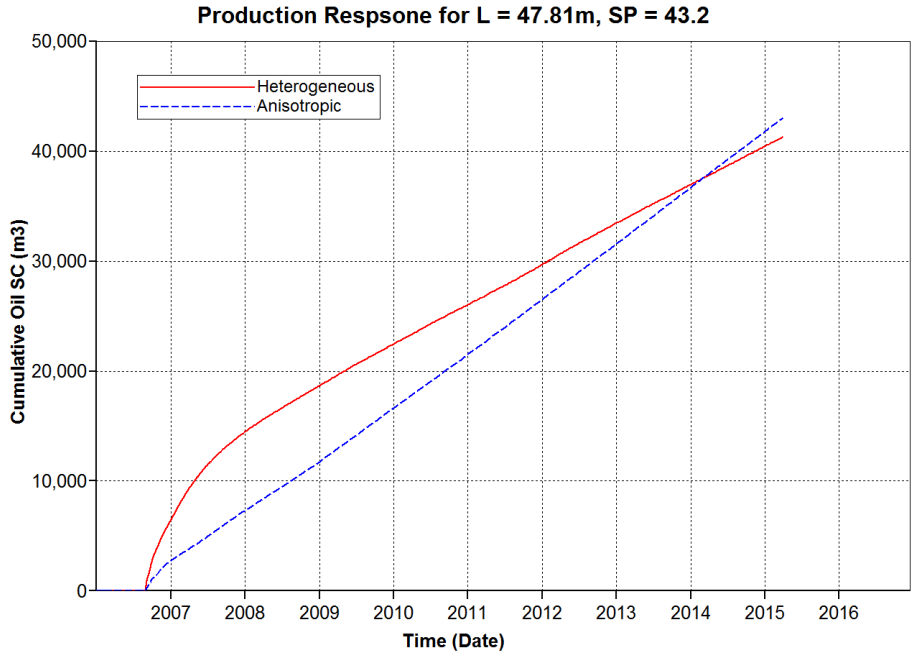

Figure 5.8: Heterogeneous vs. Anisotropic production response for λ = 47.81m, SP = 43.2%

Table 5.8: Newly optimized K_V and K_H for modified 3D surface

Length (m)	Shale Propor. (%)	Vol. (m3) Oil Recov. Heterog.	$\frac{k_v}{k_h}$ earlier from Initial 3D Surface	$k_{h,earlier}$ from Initial 3D Surface	Initial $k_{v,earlier}$ (mD)	Vol. (m3) Oil Recov. Using earlier $\frac{k_v}{k_h}$	New $k_{v,optimal}$ (mD)	New $k_{h,optimal}$ (mD)	Vol. (m3) Oil Recov. using new $\frac{k_{v,optimal}}{k_{h,optimal}}$
28.91	17.68	217071	0.369	1783	663.5	161296	1051.6	1974.3	217025
35.78	28.24	124205	0.286	1135	330.9	81132	523.70	1134.9	124125
47.81	43.2	41324	0.401	448.3	190.7	43072	166.96	478.02	41300

5.2.2 Validating Modified 3D Model

The process discussed above was extended to include 5 more realizations developed corresponding to the 3 chosen set of shale parameters. This was done because the stochastic models reproduce the specified shale parameters in an expected sense over several realizations. This procedure added an additional 15 points to the regression procedure. However, the addition of these additional points somewhat altered the regression procedure. With the additional data points, it was no longer feasible to fit the data using a regression expression that is 1st order in λ and 2nd order in shale proportion. A balance between going to higher order expressions and fitting the data and having too many degrees of freedom to over-fit the data is necessary. In order to arrive at the optimum form of the regression surface, 3 points were chosen at random corresponding to different combinations of shale parameters and the anisotropy parameters obtained using different polynomial expressions were compared against the optimized anisotropy parameters. The regression models that will be compared are A: 1st order in λ, 2nd order in SP and B: 2nd order in λ, 2nd order in SP. The regression surfaces for k_v/k_h and

corresponding k_h with respect to shale correlation length and shale proportion are shown in Figures 5.9-5.12 and the expressions that fit these models are shown in Table 5.9.

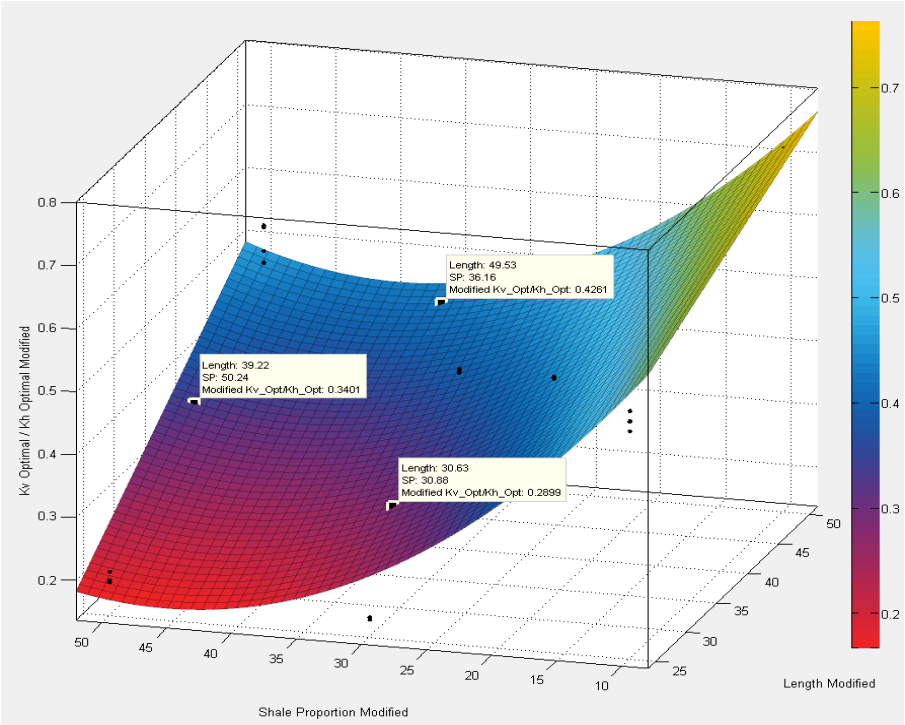

Figure 5.9: Modified regression surface that is 1st order in shale correlation length and 2nd order in shale proportion. This surface is constrained to more data compared to the surface in Figures 5.1 or 5.3.

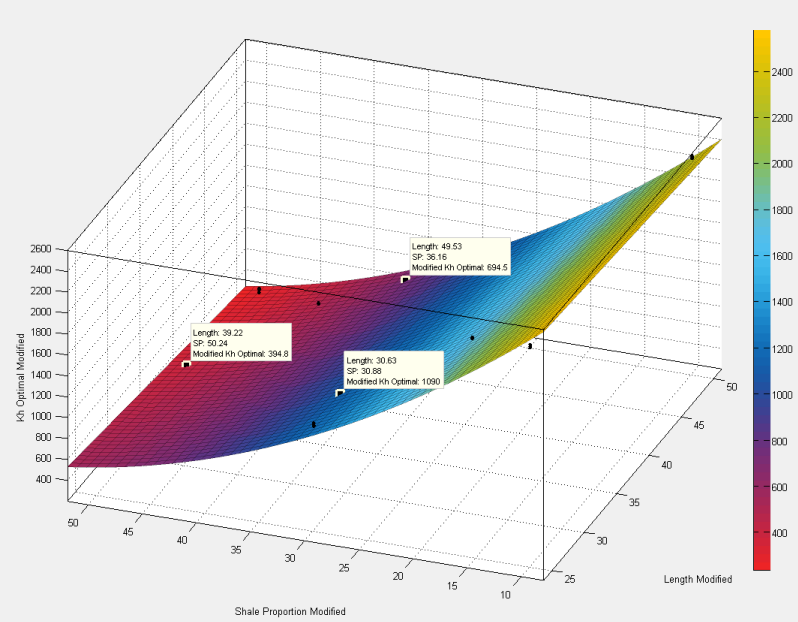

Figure 5.10: Regression surface for K_H that is 1st order in shale correlation length and 2nd order in shale proportion . This surface is constrained to more data than the earlier models in Figures 5.2 and 5.4.

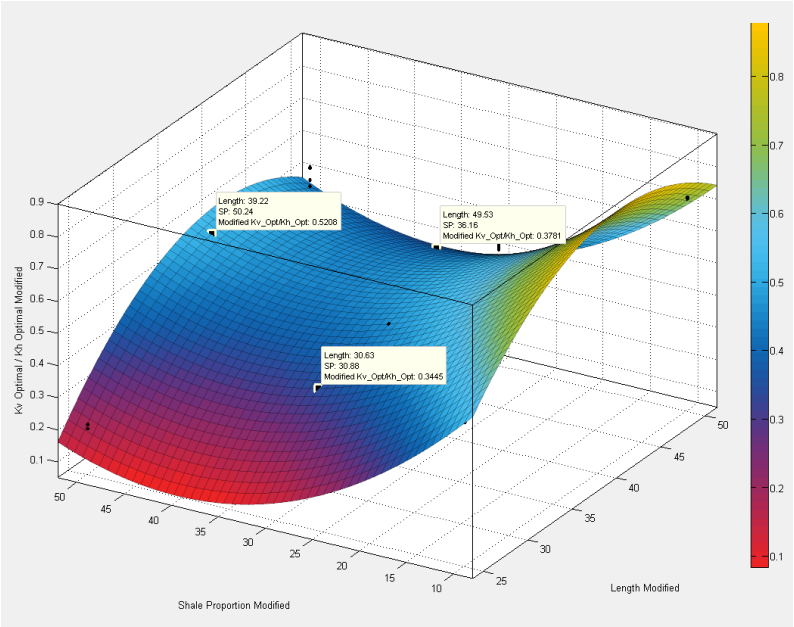

Figure 5.11: Modified regression surface for K_V/K_H that is 2nd order in shale correlation length and 2nd order in shale proportion.

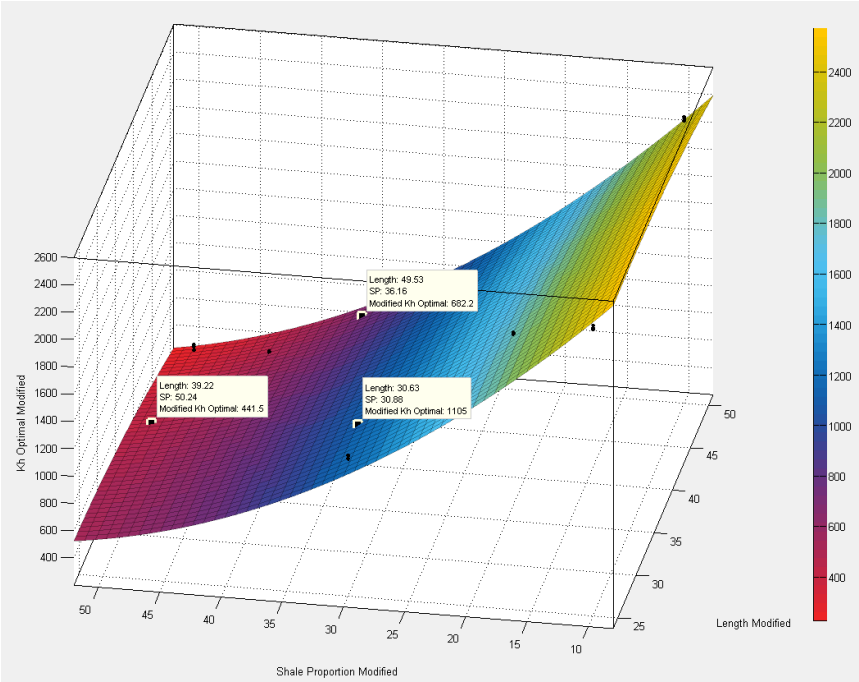

Figure 5.12: Modified regression surface for K_H that is 2nd order in shale correlation length and 2nd order in shale proportion.

Table 5.9: Expressions for the two regression surfaces used to fit the relationship between shale correlation length, proportion and anisotropic permeability values K_H and K_V/K_H

Model A: 1st Order λ, 2nd Order SP: $Z = p_{00} + \lambda * p_{10} + SP * p_{01} + \lambda * SP * p_{11} + SP^2 * p_{02}$					
Z	p_{00}	p_{10}	p_{01}	p_{11}	p_{02}
$\frac{k_v}{k_h}$	0.6934	0.004919	-0.03115	0.0001138	0.0003148
k_h	3403	-5.761	-89.52	-0.09654	0.7551

Table 5.9 Continued						
Model B: 2nd Order λ, 2nd Order SP: $Z = p_{00} + \lambda * p_{10} + SP * p_{01} + \lambda^2 * p_{20} + \lambda * SP * p_{11} + SP^2 * p_{02}$						
Z	p_{00}	p_{10}	p_{01}	p_{20}	p_{11}	p_{02}
$\frac{k_v}{k_h}$	-0.7539	0.09427	-0.0396	-0.001175	$8.494e^{-05}$	0.0004782
k_h	3028	17.35	-91.71	-0.3039	-0.104	0.7973

Naturally, with differing expressions that fit the new modified 3D model the corresponding outputs obtained using these expressions corresponding to different shale parameters will be different as well. Table 5.10 outlines these different outputs for 3 randomly selected sets of shale parameters. After determining k_v by simply multiplying $\frac{k_v}{k_h}$ with k_h, these values were specified as input for the flow simulation to see which method produced the closest match to the respective heterogeneous responses.

It was found that the production response curves for models that used optimal k_v/k_h generated by Model B where λ and SP were both of 2nd order produced the best matches to the corresponding heterogeneous response. All 3 points chosen were within 3% error of the heterogeneous value which is quite accurate for a regression based approach. Figures 5.13-5.15 displays the cumulative oil recovery using anisotropic models A and B in comparison to the heterogeneous model response. As observed before,

Model B response is closer to the heterogeneous model response. Table 5.11 displays the error between the models.

We can conclude that a highly non-linear regression model (such as in Model B) can accurately yield anisotropic permeability parameters corresponding to stochastic shale distributions in heterogeneous media. This model can be used in the simplified oil recovery expression such as proposed by Azom () to predict the performance of the SAGD process in heterogeneous systems characterized by anisotropic parameters.

Table 5.10: Optimal K_V and K_V/K_H calculated using Models A and B from Table 5.9

Point	Length (m)	Shale Proportion (%)	$\frac{k_v}{k_h}$ predicted by Model A $\{\lambda^1, SP^2\}$	$\frac{k_v}{k_h}$ predicted by Model B $\{\lambda^2, SP^2\}$	k_h predicted by Model A $\{\lambda^1, SP^2\}$ (mD)	k_h predicted by Model B $\{\lambda^2, SP^2\}$ (mD)
1	30.63	30.88	0.290	0.345	1090	1105
2	39.22	50.24	0.340	0.521	394.8	441.5
3	49.53	36.16	0.426	0.378	694.5	682.2

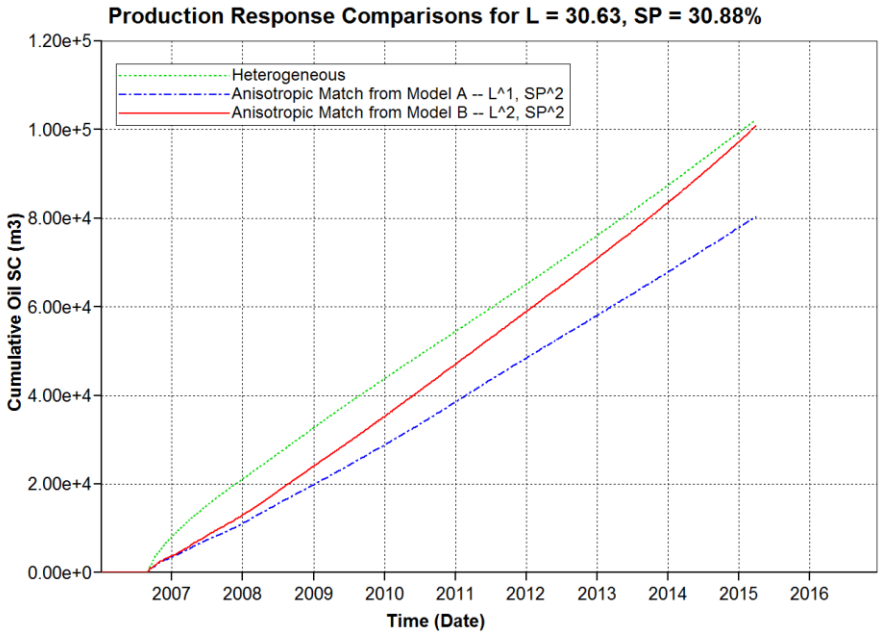

Figure 5.13: Heterogeneous vs. Anisotropic production responses for λ = 30.63m, SP = 30.88% using Model A $\{\lambda^{1}, SP^{2}\}$ and Model B $\{\lambda^{2}, SP^{2}\}$

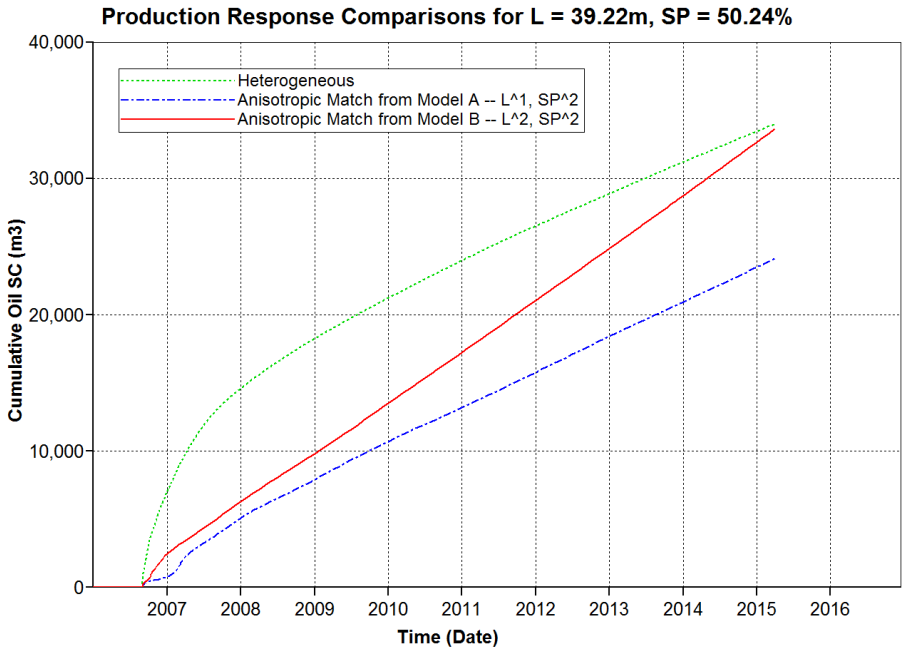

Figure 5.14: Heterogeneous vs. Anisotropic production responses for λ = 39.22m, SP = 50.24% using Model A $\{\lambda^{1}, SP^{2}\}$ and Model B $\{\lambda^{2}, SP^{2}\}$

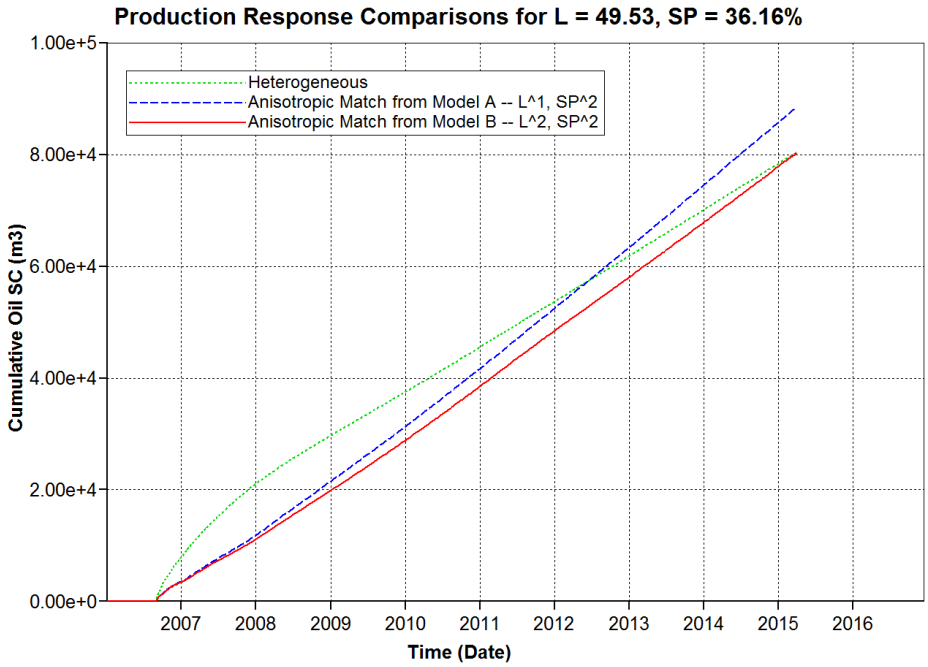

Figure 5.15: Heterogeneous vs. Anisotropic production responses for λ = 49.53m, SP = 36.16% using Model A $\{\lambda^1, SP^2\}$ and Model B $\{\lambda^2, SP^2\}$

Table 5.11: % Error in prediction between the response of the fully heterogeneous Model, anisotropic Model A and anisotropic Model B.

Point	Length (m)	Shale Proportion (%)	Vol. (m3) Oil Recov. Heterogeneous	Vol. (m3) Oil Recov. Model A $\{\lambda^1, SP^2\}$	% Error	Vol. (m3) Oil Recov. Model B $\{\lambda^2, SP^2\}$	% Error
1	30.63	30.88	102306	80359	21.45%	100910	1.36%
2	39.22	50.24	34026	25125	26.16%	33651	1.10%
3	49.53	36.16	80397	88443	10.01%	80359	~ 0

Chapter 6: Conclusions and Future Work

6.1 CONCLUSIONS

This thesis presents different methods to quantify the effect of stochastic distribution of shale in a reservoir on the performance of the SAGD process by computing effective anisotropic permeability values. Accomplishing accurate predictions using full scale heterogeneous reservoir models is computationally inefficient and so the need arises to develop equivalent anisotropic reservoirs that can demonstrate similar behavior.

Since SAGD is highly controlled by the permeability in the reservoir, effective permeability values were determined using different upscaling techniques. First, a flow-based upscaling technique was employed and a semi-analytical model derived by Azom and Srinivasan was used to determine the accuracy of the upscaling. This revealed some inadequacies with current upscaling methods for calculating effective flow properties for the SAGD process. Then statistical upscaling was employed on full 3D models to determine relationships between k_v/k_h, correlation length and proportion of shale present. An iterative procedure coupled with the GRG2 algorithm used in Microsoft Excel's Solver function was deployed to determine optimal k_v and k_h values. Then using the optimized values, the three variables were plotted in 3-dimensional space to determine a surface that could be regressed to fit the relationship that was found. These led to the following main conclusions:

- Correlation length and shale proportion play a large role in the performance of the SAGD process. Increased correlation lengths and increased shale proportions both decrease the dimensionless flow rates at a given dimensionless time.
- Azom and Srinivasan's model (2011) based on an extension of Butler's model (1981) was more accurate for models that contained lower shale proportions.

Upscaling heterogeneous values for input into an analytic model, such as Azom's model, will result in an overestimate of flow rate due to the inability to fully account for the impact of reservoir barriers and the configuration of flow streamlines during the SAGD process.

- Simulation results suggest the importance of steam chamber shape in the estimation of flow rates especially when compared to rates predicted by analytical models.
- Statistical upscaling schemes were employed on full heterogeneous models and converged values of k_v and k_h were determined such that the volume of oil recovered matched initial heterogeneous model. Statistical upscaling using geometric averaging produced the best initial guess to the heterogeneous model while harmonic averaging severely underestimated performance and arithmetic averaging overestimated performance.
- A non-unique relationship between k_v/k_h and cumulative oil recovered was observed leading to the conclusion that the individual values of k_v and k_h play a more significant role on recovery than the corresponding ratio.
- When fitting a 3D surface that modeled relationship between length, shale proportion and optimal values of k_v/k_h, it was found that when an arbitrary length and shale proportion was chosen the initial 3D model did not accurately match the heterogeneous model with the same parameters. It was believed that this was because of insufficient data points along the regression surface causing inaccuracies. Updated optimal values for k_v and k_h values were then added to the initial regression model in order to improve the predictive accuracy of the regression model. Since there were now more points on the regression surface, the expression used to model the surface could contain higher order terms. To

determine the exact combination of variable orders, different combinations were tested and it was found that the expression that was 2nd order in both length and shale proportion produced excellent matches to heterogeneous models for the cases that were chosen.

- The results suggest a strong non-linear relationship between the shale parameters and the corresponding effective permeability values.

6.2 FUTURE WORK

One of the principal limitations of the statistical upscaling schemes was that it did not mimic the actual behavior of the fully heterogeneous model. For example, any case with an optimized permeability ratio that produced a good match to the heterogeneous model it was upscaled from exhibit a strong mismatch at early times but converge to the same final cumulative oil output. An example of this can be seen in Figure 4.6. If this response was observed, the initial mismatch is so large that it could lead to an incorrect estimation of the final production value and the reservoir in question may be abandoned.

Several attempts were made to minimize this initial difference, however no combination of effective permeability values produced a match in production responses. Reservoirs were separated into different regions based on steam chamber growth and spread with different permeability values in each region in an attempt to account for the initial mismatch, however each case resulted in a severe overestimation of the reservoir heterogeneity. More work should be performed to determine a method to minimize the difference between the two production profiles to further improve the current statistical relationship between correlation length, shale proportion and permeability.

Appendix

Table A1: Upscaled Permeability Values

	Kh	Avg. Kh	Kv	Avg. Kv	Kv/Kh	Avg. Kv/Kh
L5_Fm	772.96	722.69	434.51	401.04	0.562	0.560
	739.12		383.23		0.518	
	746.48		386.08		0.517	
	577.56		383.25		0.664	
	777.33		418.11		0.538	
L15_Fhi	187.53	249.89	48.74	61.15	0.260	0.264
	156.69		75.37		0.481	
	395.23		99.89		0.253	
	186.71		32.26		0.173	
	323.31		49.48		0.153	
L15_Flo	1717.28	1661.06	1168.34	993.30	0.680	0.597
	1694.54		1059.02		0.625	
	1606.85		891.89		0.555	
	1709.28		949.11		0.555	
	1577.34		898.14		0.569	
L15_Fm	816.68	910.66	351.65	294.31	0.431	0.334
	1019.13		238.43		0.234	
	922.09		261.05		0.283	
	773.50		367.08		0.475	
	1021.90		253.36		0.248	
L25_Fhi	389.45	415.57	53.47	47.52	0.137	0.115
	511.46		50.28		0.098	
	338.37		30.38		0.090	
	443.63		49.51		0.112	
	394.94		53.97		0.137	
L25_Flo	1712.83	1692.53	1161.09	1082.68	0.678	0.639
	1733.96		1335.80		0.770	
	1696.11		937.80		0.553	
	1698.34		975.86		0.575	
	1621.42		1002.86		0.619	
L25_Fm	813.51	874.57	177.27	192.16	0.218	0.212
	878.51		133.62		0.152	
	719.12		224.07		0.312	
	1263.85		358.31		0.284	
	697.85		67.55		0.097	

Table A1 Continued						
L35_Fm	963.29	938.78	163.65	209.88	0.170	0.228
	1113.22		155.69		0.140	
	792.27		79.23		0.100	
	700.46		278.35		0.397	
	1124.66		372.49		0.331	

Table A2: Additional Simulation Parameters

Volumetric heat capacity	1593.3 kJ/m^2·^{o}C
Bitumen density	1023 kg/m^3
Reservoir thickness	1 m
Initial oil saturation	1.0
Initial water saturation	0.0
Initial steam saturation	0.0
Reference pressure	1958 kPa
Reference temperature	225 ^{o}C
Max simulation time	3000 days

```
Sub RangeLoop1()
  Dim i As Integer
   Dim j As Integer
   Dim h As Integer
   For i = 1 To 2000
     For j = -2000 To j = 0
     If ActiveCell.Offset(0, -4).Value = ActiveCell.Offset(j, -8).Value Then
ActiveCell.Value = ActiveCell.Offset(0, -4).Value
     If ActiveCell.Offset(0, -4).Value = ActiveCell.Offset(j, -8).Value Then
ActiveCell.Offset(0, 1).Value = ActiveCell.Offset(0, -2) / ActiveCell.Offset(j, -6).Value
     Next j
     For h = -2000 To h = -1
     If ActiveCell.Offset(0, -4).Value = ActiveCell.Offset(-h, -8).Value Then
ActiveCell.Value = ActiveCell.Offset(0, -4).Value
     If ActiveCell.Offset(-h, -6).Value = 0 Then ActiveCell.Offset(-h, -6).Value = 0.01
     If ActiveCell.Offset(0, -4).Value = ActiveCell.Offset(-h, -8).Value Then
ActiveCell.Offset(0, 1).Value = ActiveCell.Offset(0, -2) / ActiveCell.Offset(-h, -6).Value
     Next h
   ActiveCell.Offset(1, 0).Select
   Next i
End Sub
```

Figure A1: VBA Code for determining exact dimensionless time matches

```
Sub Wsd()
   For j = 1 To 50
      For i = 1 To 5
         ActiveCell.EntireRow.Delete
      Next i

      temp = j * 150 - 149
      Cells(temp, 1).Select
      For k = 1 To 150
         ActiveCell.Value = j
         ActiveCell.Offset(1, 0).Select
      Next k

   Next j

End Sub
Sub avg()
   Sum = 0
   Tots = 0
   For i = 1 To 7500

      If ActiveCell.Value <= 0.9 Then
      Sum = Sum + ActiveCell.Value
      Tots = Tots + 1
      End If

   ActiveCell.Offset(1, 0).Select
   Next i

   Cells(1, 5).Value = Sum
   Cells(1, 6).Value = Tots
   Cells(1, 7).Value = Sum / Tots
End Sub
```

Figure A2: VBA Code for determining oil saturation inside Steam Chamber

Table A3: Anisotropic k_v/k_h to match Heterogeneous Output – Arithmetic Upscaling

Correlation Length (m)	Shale Proportion (%)	Heterogeneous Cumulative Oil Output (m3)	Initial k_v/k_h Guess	Actual k_v/k_hvia Solver	Cumulative Oil (m3) using Solver k_v/k_h	Error (%)
25	50%	30,485	0.52	0.042	31028.6	1.83
25	30%	62,810	0.679	0.076	62799.7	0.097
25	10%	232,850	0.873	0.364	232451	0.218
50	50%	32,159	0.729	0.051	35129	0.215
50	30%	81,573	0.829	0.105	78440.7	3.83
50	10%	248,659	0.935	0.515	249,250	~ 0

Table A4: Initial Guesses of kv/kh and Corresponding Cumulative Oil Recovered in Comparison to Fully Heterogeneous Model

			Initial kv/kh Guesses and Corresponding Cumulative Oil Recovered					
Correlation Length	Shale Proportion	Heterog. Output	Arith kv/kh	Arith Cum. Oil Output (m3)	Geom. kv/kh	Geometric Cum. Oil (m3)	Harm. kv/kh	Harm. Cum. Oil (m3)
25	50%	69359	0.825	248844	0.312	77776	0.612	382
25	30%	62810	0.679	238498	0.161	66815	0.340	396
25	10%	232960	0.873	284888	0.45	224282	0.246	25646
50	50%	32159	0.523	181411	0.448	24367.5	0.485	366
50	30%	81573	0.829	249987	0.384	80250.8	0.607	383
50	10%	248659	0.935	285204	0.726	226425	0.523	19429

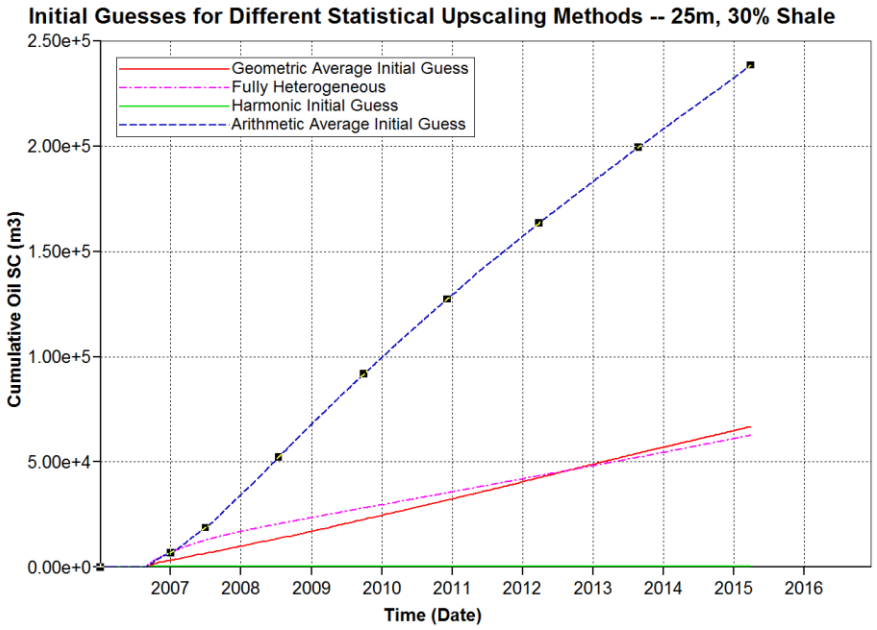

Figure A3: Initial Guesses for Different Statistical Upscaling Schemes for 25m, 30% Shale

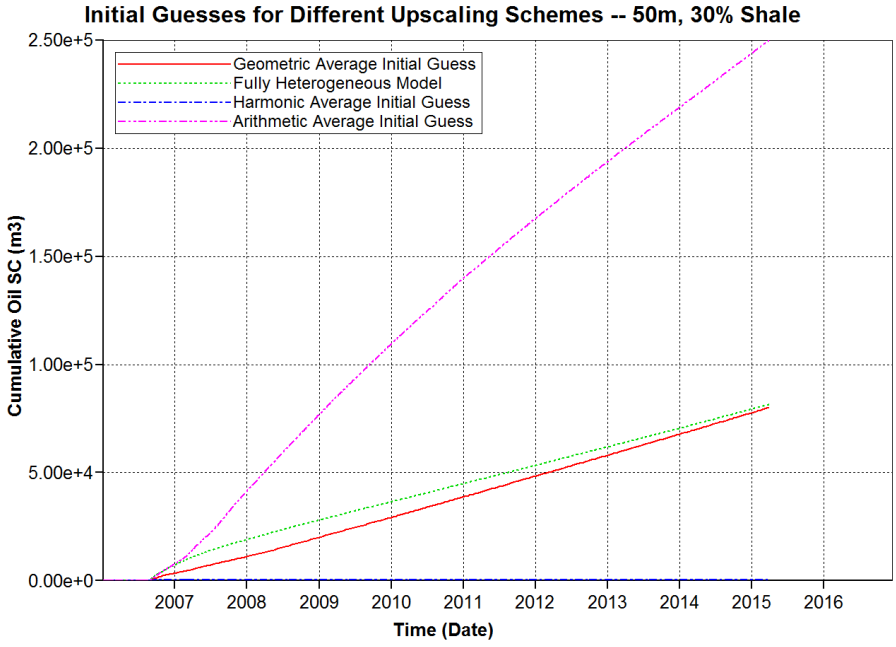

Figure A4: Initial Guesses for Different Statistical Upscaling Schemes for 50m, 30% Shale

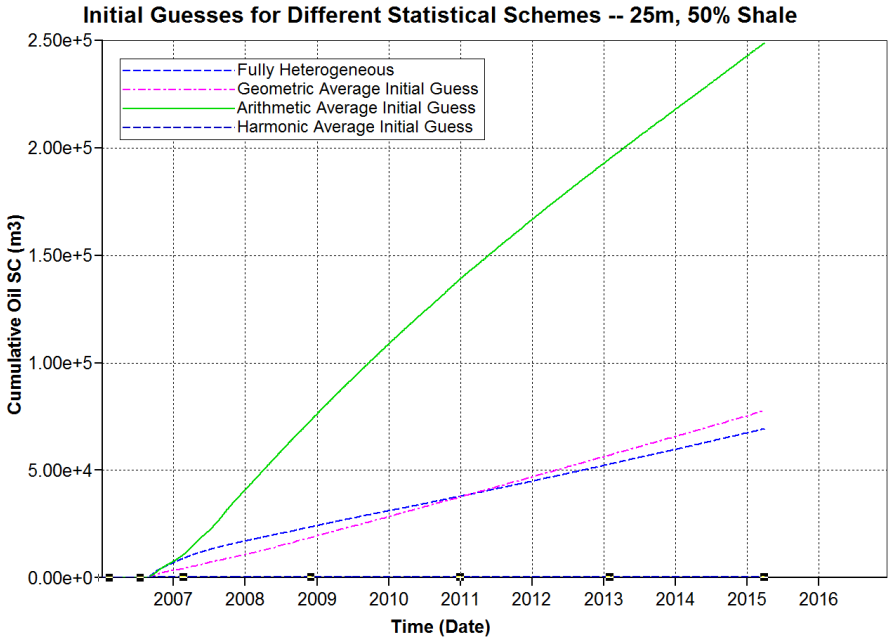

Figure A5: Initial Guesses for Different Statistical Upscaling Schemes for 25m, 50% Shale

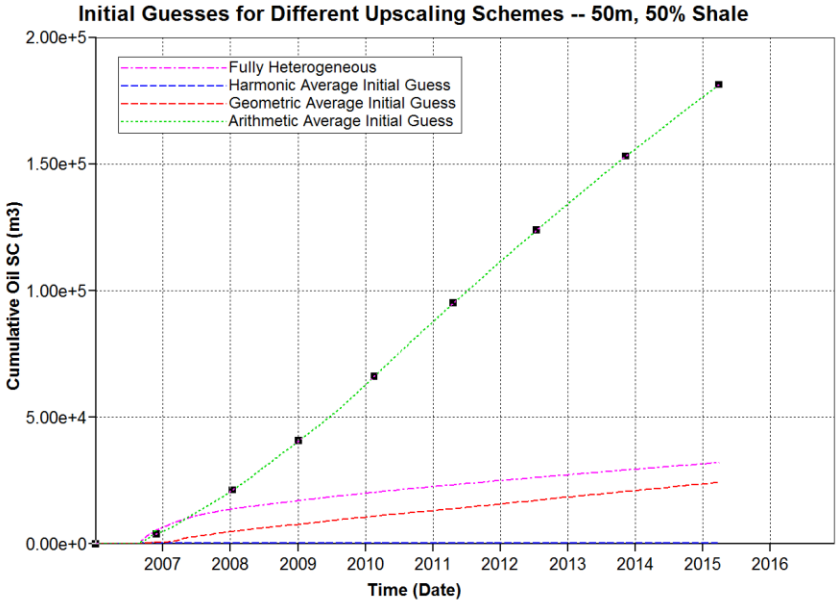

Figure A6: Initial Guesses for Different Statistical Upscaling Schemes for 50m, 50% Shale

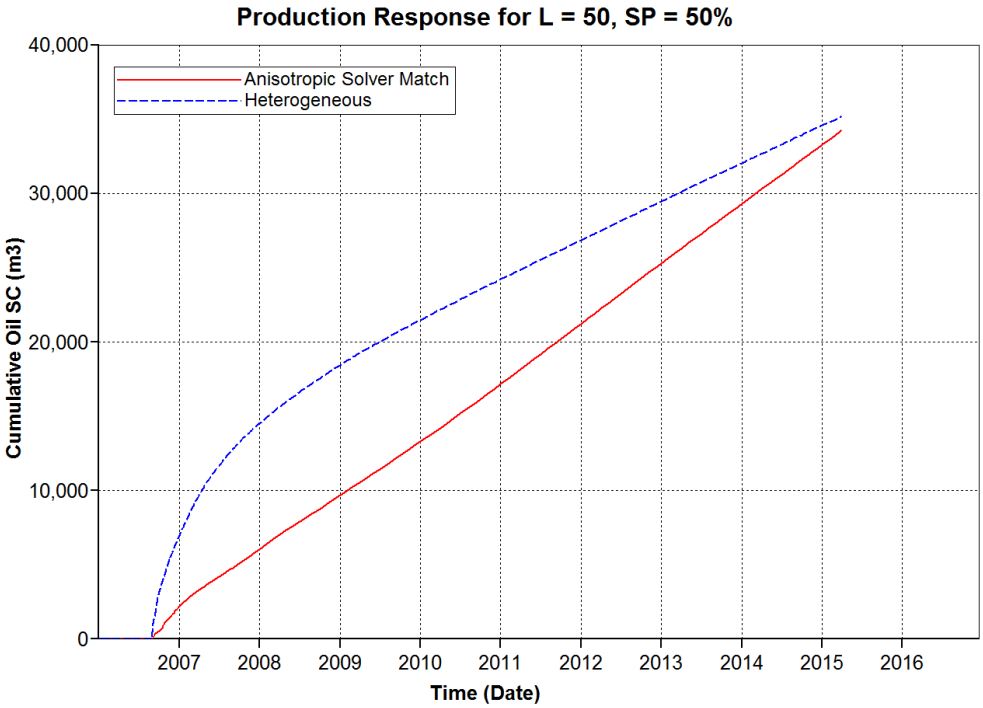

Figure A7: Heterogeneous vs. Anisotropic solver match for λ = 50m, SP = 50%

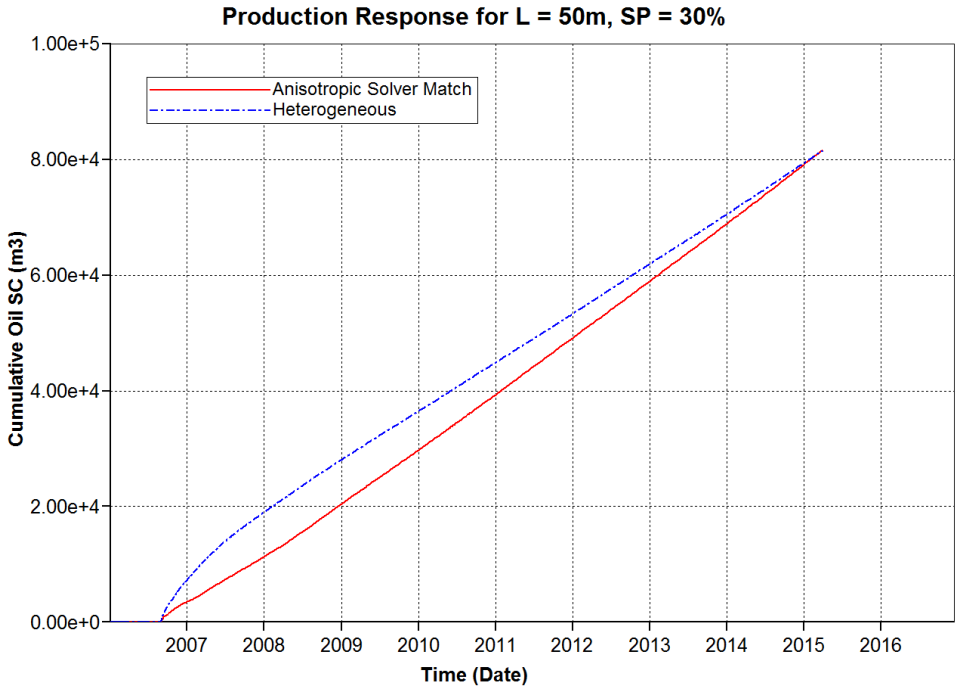

Figure A8: Heterogeneous vs. Anisotropic solver match for λ = 50m, SP = 30%

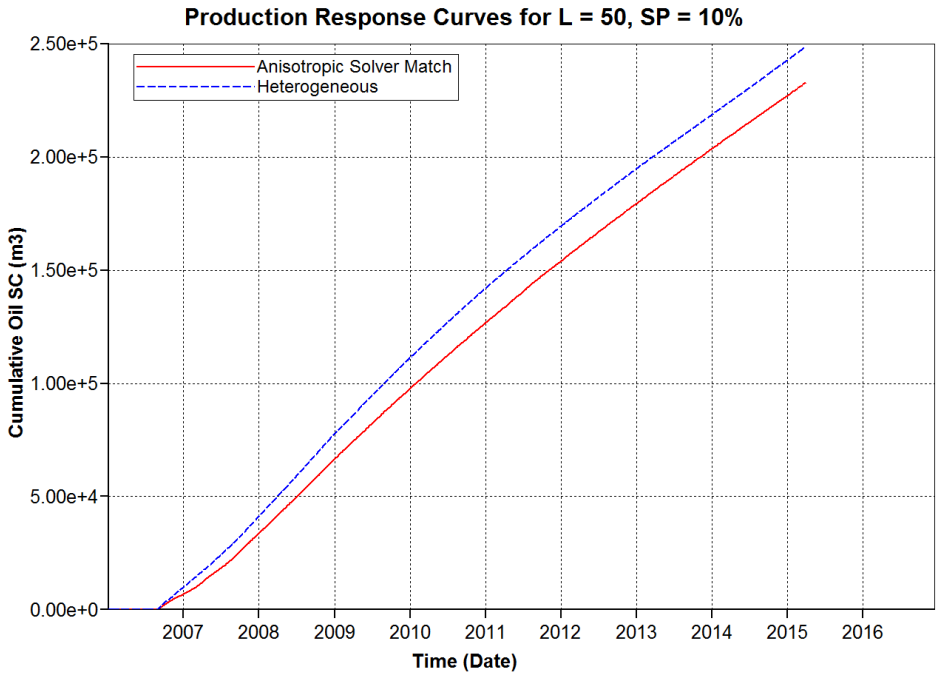

Figure A9: Heterogeneous vs. Anisotropic solver match for λ = 50m, SP = 10%

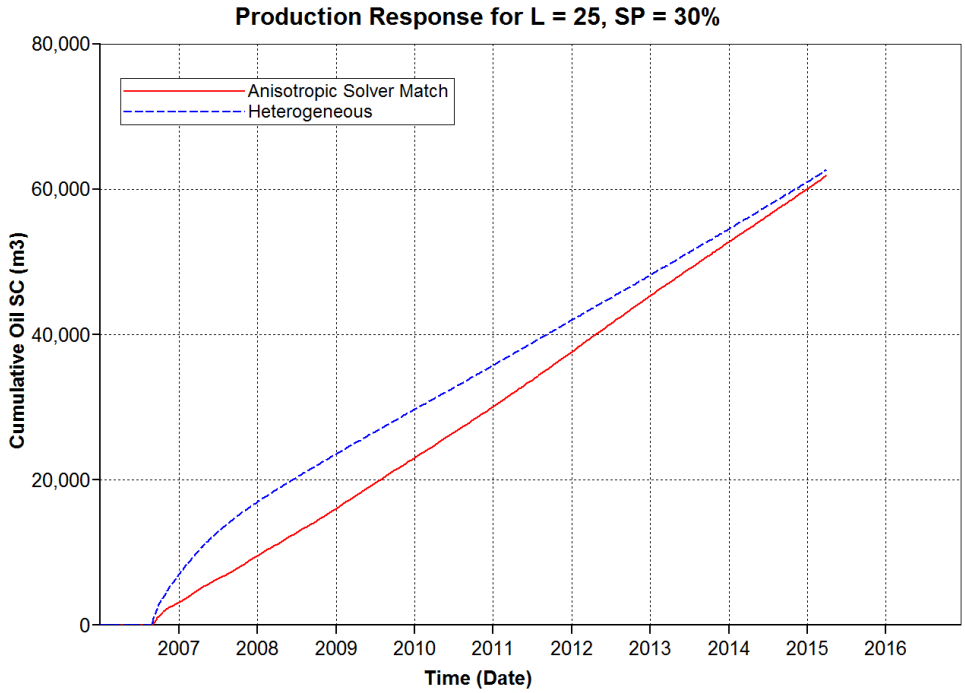

Figure A10: Heterogeneous vs. Anisotropic solver match for λ = 25m, SP = 30%

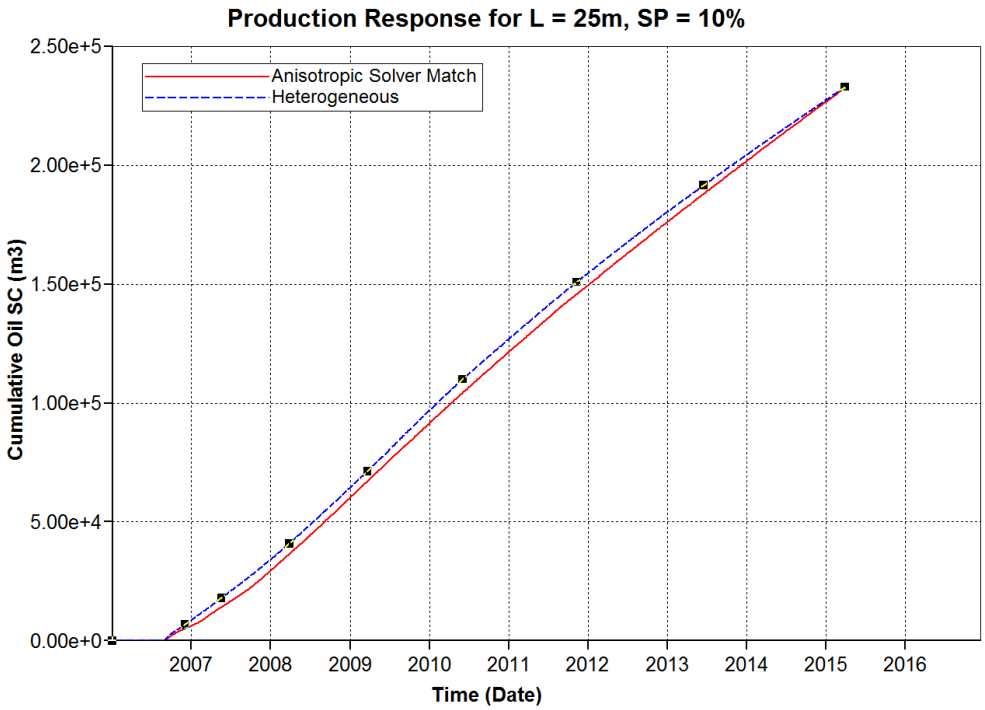

Figure A11: Heterogeneous vs. Anisotropic solver match for λ = 25m, SP = 10%

References

Alali, N., Pishvaie, M.R., Jabbari, H., 2009. A new semi-analytical modeling of steam-assisted gravity drainage in heavy oil reservoirs. Journal of Petroleum Science and Engineering 69, 261–270.

Anand, J., Somerton, W.H., Gomaa, E. 1973. Predicting Thermal Conductivities of Formations from Other Known Properties. Society of Petroleum Engineers Journal, Vol. 13, No. 5, pp. 267-273.

Azad, A., 2012. Rapid SAGD Simulation Simulation Considering Geomechanics for Closed Loop Reservoir Optimization, PhD Dissertation, University of Alberta, Alberta, Canada.

Azom, P.N. Improved Modeling of The Steam-Assisted Gravity Drainage (SAGD) Process. Dissertation, University of Texas, Austin, 2012.

Azom, P.N., Srinivasan, S. 2011. Modeling the Effect of Permeability Anisotropy on the Steam-Assisted Gravity Drainage (SAGD) Process. Canadian Unconventional Resources Conference, SPE, Alberta, Canada, November 2011.

Bakr, A, A., Gelhar, L. W., Gutjahr, A. L., and MacMillan, J. R., 1978, Stochastic Analysis of Spatial Variability in Subsurface Flows 1. Comparison of One- and Three-Dimensional Flows: Water Resour. Res., v. 14, p. 263-271.

Barillas, J.L.M., Dutra Jr., T.V., Mata, W., 2006. Reservoir and operational parameters influence in SAGD process. Journal of Petroleum Science and Engineering 54, 34–42.

Begg, S.H., Chang, D.M., 1985. A Simple Statistical Method for Calculating the Effective Vertical Permeability of a Reservoir Containing Discontinuous Shales. Society of Petroleum Engineers.

Butler, R., 1985. A New Approach To The Modelling of Steam-Assisted Gravity Drainage. Journal of Canadian Petroleum Technology.

Butler, R., Mokrys, I., 1991. A New Process (VAPEX) For Recovering Heavy Oils Using Hot Water And Hydrocarbon Vapour. Journal of Canadian Petroleum Technology.

Butler, R.M. 1985. A New Approach to Modeling of Steam-Assisted Gravity Drainage. Journal of Canadian Petroleum Technology, Vol. 24, No. 3, pp. 42-51.

Butler, R.M., Mcnab, G.S., Lo, H.Y., 1981. Theoretical studies on the gravity drainage of heavy oil during in-situ steam heating. The Canadian Journal of Chemical Engineering 59, 455–460.

Chen, Q., Gerritsen, M., Kovscek, A., 2008. Effects of Reservoir Heterogeneities on the Steam-Assisted Gravity-Drainage Process. SPE Reservoir Evaluation & Engineering 11.

CMG. 2011. CMG-STARS User Manual.

Dagan, G., 1979, Models of Groundwater Flow in Statistically Homogeneous Porous Formations: Water Resour. Res., v. 15, p. 47-63.

Dagan, G., 1981, Analysis of Flow Through Heterogeneous Random Aquifers by the Method of Embedding Matrix 1. Steady Flow: Water Resour. Res., v. 17, p. 107-121.

Das, Braja M. 2013. *Advanced Soil Mechanics*. 4th ed. Crc Pr I Llc.

Desbarats, A. J., 1987, Numerical Estimation of Effective Permeability in Sand-Shale Formations: Water Resour. Res,, v. 23, p. 273-286.

Deutsch, C., 2010. Estimation of Vertical Permeability in the McMurray Formation. Journal of Canadian Petroleum Technology 49.

Deutsch, C.V., Journel, A.G. 1998. GSLIB. Geostatistical Software Library and User's Guide, 2nd ed.

Duong, A.N., Tomberlin, T.A., Cryot, M. 2008. A New Analytical Model for Conduction Heating During the SAGD Circulation Phase. SPE/PS/CHOA International Thermal Operations & Heavy Oil Sym., Alberta, Canada.

Durlofsky, L.J. 1991. Numerical Calculation of Equivalent Grid Block Permeability Tensor for Heterogeneous Porous Media. Water Resources Research, Vol. 27, No. 5, pp. 699-708.

Haldorsen, H., Lake, L., 1984. A New Approach to Shale Management in Field-Scale Models. Society of Petroleum Engineers Journal 24.

Japan Exploration's website page www.japex.co.jp/english/business/oversea/sagd.html

Jensen, J.L. Use of the Geometric Average for Effective Permeability Estimation. 1991. Mathematical Geology 23, 833—840.

Kamath, V.A., Sinha, S., Hatzignatiou, D.G. 1993. Simulation Study of Steam-Assisted Gravity Drainage Process in Ugnu Tar Sand Reservoir. SPE Western Regional Meeting, Anchorage, Alaska, May 1993.

Kamath, V.A., Sinha, S., Hatzignatiou, D.G., 1993. Simulation Study of Steam-Assisted Gravity Drainage Process in Ugnu Tar Sand Reservoir. Society of Petroleum Engineers.

Kisman, K.E., Yeung, K.C., 1995. Numerical Study of the SAGD Process in the Burnt Lake Oil Sands Lease. Society of Petroleum Engineers.

Kou, J., Wu, F., Lu, H, Xu, Y., Song, F. 2009. The Effective Thermal Conductivity of Porous Media Based on Statistical Self-Similarity. Physics Letters A, Vol. 374, pp. 62-65.

Le Ravalec, M., Morlot, C., Marmier, R., Foulon, D. 2009. Heterogeneity Impact on SAGD Process Performance in Mobile Heavy Oil Reservoirs. Oil & Gas Science and Technology, Vol. 64, No. 4, pp. 469-476.

Le Ravalec, M., Morlot, C., Marmier, R., Foulon, D., 2009. Heterogeneity Impact on SAGD Process Performance in Mobile Heavy Oil Reservoirs. Oil & Gas Science and Technology - Revue de l'IFP 64, 469–476.

Llaguno, P., Moreno, F., Garcia, R., Mendez, Z., Escobar, E., 2002. A Reservoir Screening Methodology for SAGD Applications. Society of Petroleum Engineers.

Luo, M., Wood, J., Cathles, Lawrence M. 1994. Prediction of Thermal Conductivity in Reservoir Rocks Using Fabric Theory. Journal of Applied Geophysics, Vol. 32, pp. 321-334.

Matheron, G., t967, Elements Pour une Theorie des Milieux Poreux, Masson et Cie, Paris, 166 p.

McLennan, J., Deutsch, C., Garner, D., Mus, E., Wheeler, T., Richy, J.-F., 2006. Permeability Modeling for the SAGD Process Using Minimodels. Society of Petroleum Engineers.

Meyer, R. F., E. D. Attansasi, and P. A. Freeman. 2007. Heavy Oil and Natural Bitumen Resources in Geological Basins of the World. Open File. US Geological Survey.

Najeh, A., Pishvaie, R.M., Jabbari, H. 2009. A New Semi-Analytical Modeling of Steam-Assisted Gravity Drainage in Heavy Oil Reservoirs. Journal of Petroleum Science and Engineering, Vol. 69, pp. 261-270.

Peaceman, D.W., 1993. Reperesentation of a Horizontal Well in Numerical Reservoir Simulation. SPE Advanced Technology Series 1.

Remy, N. 2008. Applied Geostatistics with SGeMS: A User's Guide.

Sharma, B., Santanu, K., Patil, S., Kamath, V., Dandekar, A., 2002. A Simulation Study of Novel Thermal Recovery Methods in the Ugnu Tar Sand Reservoir, North Slope, Alaska. Society of Petroleum Engineers.

Sharma, J., Gates, I. 2010. Multiphase Flow at the Edge of a Steam Chamber. The Canadian Journal of Chemical Engineering, Vol. 88, pp. 312-321.

Shin, H., Choe, J., 2009. Shale Barrier Effects on the SAGD Performance. Society of Petroleum Engineers.

Warren, J.E., Price, H.S. 1961. Flow in Heterogeneous Porous Media. Society of Petroleum Engineers Journal 03, 153—169.